NATIONAL ADVISORY COMMITTEE FOR AERONAUTICS

WARTIME REPORT

ORIGINALLY ISSUED

January 1943 as

Advance ████████ Report

FLIGHT INVESTIGATION OF NACA D_S COWLINGS ON THE

XP-42 AIRPLANE. I - HIGH-INLET-VELOCITY

COWLING WITH PROPELLER CUFFS TESTED

IN HIGH-SPEED LEVEL FLIGHT

By F. J. Bailey, Jr., and J. Ford Johnston

Langley Memorial Aeronautical Laboratory
Langley Field, Va.

FILE COPY

NACA

WASHINGTON

NATIONAL ADVISORY COMMITTEE FOR AERONAUTICS

ADVANCE ██████████ REPORT

FLIGHT INVESTIGATION OF NACA D_S COWLINGS ON THE

XP-42 AIRPLANE. I - HIGH-INLET-VELOCITY

COWLING WITH PROPELLXR CUFFS TESTED

IN HIGH-SPEED LEVEL FLIGHT

By F. J. Bailey, Jr., and J. Ford Johnston

SUMMARY

Results are presented of a series of flight tests of the maximum speed and? cooling characteristics in full-throttle level. flight of the XP-42 airplane equipped with a short-nose high-inlet velocity cowling. This cowling is one of a series being tested in an effort to improve the performance and cooling characteristics of air-cooled engine installations.

The results of the tests indicated a maximum speed of 336 miles per hour at 960 horsepower at 25,000 feet.

Pressure measurements in the entrances to the cylinder baffles showed a fairly uniform distribution of pressure around the engine at similar points of measurement on individual cylinders but indicated that cooling-air pressures varied considerably for different points of measurement on the same cylinder, Tho variation was probably due to t'e velocity head of the entering cooling-air jet. Static pressure behind the engine was uniform.

Front pressures on the engine averaged 80 percent and rear pressures 39 percent of free-stream impact pressure. The resulting pressure drop of 15 inches of water at full throttle at 15,000 feet cooled the cylinder heads adequately; maximum cylinder base temperatures, however, exceeded the specified limits when corrected to Army summer conditions.

Pressure measurements in the carburetor and oil-cooler ducts showed rams of slightly over 100 percent of free-stream impact pressure, Air-flow measurements in the car-

buretor duct and in the annular entrance to the engine
compartment showed that the volume flows of induction and
cooling air were approximately constant at full throttle
over a range of altitudes near the critical altitude and
were, respectively, 2960 and 19,900 cubic feet of free air
per minute.

INTRODUCTION

The National Advisory Committee for Aeronautics is in-
vestigating means of modifying the conventional NACA radial
engine cowling to meet the demands imposed by the latest
designs of military airplanes. Tests in a number of the
wind tunnels have been directed. toward improving the cowl-
ing in the follomiiig respects:

1. Greater stability of the air flow within the cowl-
ing, particularly at angles of attack corresponding to the
climb condition, to provide a uniform cooling-air pressure
in front of tne engine

2. Reduction of energy losses in the cooling air in
front of the engine by the use of an efficient diffuser
between the inlet and the front Pace of engine

3. Adequate ground cooling characteristics

4. Improvement in the external shape to reduce drag
and to increase the critical s-peed of the cowling

The NACA D-series cowlings have been developed to
meet these requirements. The D cowlings are character-
ized by the use of a cowling inner liner and of an after-
body behind the spinner. These units form an annular en-
trance followed by a diffuser section made up of the after-
body and inner liner. Investigations such as reported in
references 1 and 2 have indicated desirable ranges of
cooling-air inlet velocities, diffuser proportions, and
external contours.

In order to expedite incorporation of these new fea-
tures in projected designs for military aircraft, the
NACA is conducting flight tests of the Curtiss XP-42 air-
plane fPtted with several engine installations utilizing
the latest developments of the BACA cowling and individ-
ual cylinder jet exhaust stacks (reference 3).

The XP-42 airplane is powered by a Pratt & Whitney
1830-31 engine. As originally furnished with the airplane,
this engine carried an extension shaft that placed the
propeller 20 inches ahead of the normal position. The
first of the cowlings included in the series of tests was
designed for this long-nose engine and represented a com-
plete redesign of the cowling furnished with the airplane.
The development of this cowling in the full-scale wind
tunnel is described in reference 2 and the flight-test re-
sults are presented in reference 4.

The present report is the first of a series of re-
ports on the short-nape (D_S) cowlings and contains the
results of bests in the high-speed level-flight condition
of the high-inlet-velocity cowling, which was designed
for t-10 short-nose Pratt & Whitney 1830 engine. This cowl-
ing was tested on the XP-42 airplane by replacing the nose-
extension shaft of the 1830-31 engine with a shaft of
standard size.

For convenience, test numbers have been assigned each
cowling arrangement and flight condition. Tests 1 and 2
were the high-speed and climb tests of the long-nose cowl-
ing and test 3 is the investigation on the short-nose
cowling reported herein. Further identification has been
given by prefixing this test number to the number for a
particular flight, which was arbitrarily assigned. For
example, flight 3-6 indicates flight 6 in which the air-
plane was in test condition 3.

It was necessary to defer the final part of the tests
of this cowling, involving determination of its cooling
characteristics in climb, until the scheduled high-speed
tests of other arrangements hac? been completed and the in-
adequate cowl flap installation could be modified as in
reference 4,

The design of the cowling nnd engine installation was
a project of the Air-Cooled Engine-Installation Group sta-
tioned at the Laboratory. The members of the group asso-
ciated with this project included Mr. Howard S. Ditsch, of
the Curtiss Wright Corporation; Mr. Peter Torraco, of the
Republic Aviation Corporation; Mr. William S. Richards, of
the Wright Aeronautical Corporation; and Mr. James R.
Thompson, of Pratt & Whitney Aircraft. The Materiel Com-
mand, Army Air Forces sponsored the investigation and sup-
plied the XP-42 airplane. The Airplane Division of the ..
Curtiss-Wright Corporation handled the construction as

well as the structural and detail design of the cowling,
and supplied personnel to assist in the servicing and
maintenance of the airplane and cowling during the **tests**,
Pratt & Whitney Aircraft prepared the engfne and torque
meter for the tests and assisted in the operation and
servicing of the engine. The propeller, **cuffs,** and spin-
ner were supplied by the Propeller Division of the Curtiss-
Wright Corporation.

This report was originally issued as a memorandum **re-**
port for the Army Air Corps.

XP-42 AIRPLANE WITH SHORT-NOSE COWLING

The XP-42 airplane is identical with the P-35 airplane
except for the fuselage fairing behind the cowling and the
installation of its Pratt & Whitney 1830 engine with its
higher critical altitude rating. The power rating of the
engine is as follows:

	Brake horsepower	Engine speed (rpm)	Altitude (ft)
Take-off	1050	2550	0
Normal rating	1000	2300	8,500
Normal rating	1000	2450	11,500
Military rating	1000	2700	14,500

The engine has a single-stage blower with an impeller-
drive ratio of 8.47:1 and a propeller-drive ratio of 9:16.
The engine-cylinder baffles were reworked to minimize the
leakage of air between adjoining baffles and to direct the
cooling air on the cylinders in an efficient manner.

The 10-inch-diameter oil cooler furnished with the
engine **was** replaced by an 11-inch U.A.P. cooler with tho
same core depth of 9 inches, Individual jet exhaust stacks
were used in place of tho standard collector ring. These
stacks are made of 0.049-inch stninless-steel tubing of
$2\frac{3}{8}$-inch outside diameter, The ends of the stacks were
flattened to reduce the internal area **from** 4.05 to 2.98
square inches.

The engine cowling and propeller cuffs were fabricated by the Curtiss—Wright Corporation and are shown in figures 1 to *6*.

The fuselage side panels reported in references **1 and** 2 were used to improve the fairing of the cowling into the fuselage. The airplane, as prepared for the tests, weighed about 6000 pounds with 175-pound pilot **and** full tanks, It retained the standard aerial, but had no provisions for guns.

TEST APPARATUS

The installation of test equipment was designed to give as nearly as possible a continuous record of the pertinent data, with the exception of air-flow measurements, throughout each flight. Continuous records were taken of airspeed., altitude, manifold pressure, engine speed and torque, and temperatures. Air **flows** were measured by recording instruments **during** the particular flight conditions under investigation.

Free—stream impact pressure was measured by an NACA airspeed recorder connected to an airspeed boom on the right wing tip (fig. 7). The boom carried *a* fixed static head about one chord Length ahead of the leading edge of the wing and a special shielded impact head halfway between the static head and the lending edge of the wing. The static head was calibrated in flight by flying at a known gecmetric height at several airspeeds with a sensitive altimeter (fig, 8) connected to the static head. The shielded impact head is accurate at all angles of attack encountered in steady flight.

Atmospheric pressure was measured by an NACA recording altimeter vented to the compartment behind the cockpit in which the recording instruments were installed. **Pressure** data so acquired were corrected for the measured difference between the compartment pressure and true static pressure.

In the same instrument was incorporated another cell that recorded absolute mnnifold pressure at the supercharger blower rim.

The **pressure** from a Pratt & Whitney oil-pressure torque meter installed in the nose of the engine was trans-

mitted both to a gage in the **pilot's** cockpit **and** to an NACA pressure recorder having a range of 400 pounds per square inch, This installation permitted both visual and recorded indications of the torque delivered to the propeller. This record, in conjunction with tha engine-speed record, permitted calculation of tha brake horsepower delivered to tho propeller at any time during the **flight.**

Engine speed was **recorded** by moans of a revolution counter tcod off tho tachometer drive. At every 200th revolution of tho ongino, a contact was made that operated a solonoid and mado a mark on tho airspeed film. Since a chronometric timer was also used to mark tho **film** every 3 soconds, the time for 200 revolutions could **bo** calculated **from** tho relative distances along the **film** of engine spcod and timor marks.

All temperature records were mado by means of thermocouple connected through two 34-position rotating switches to two-coll recording galvanometer, Tho cold junctions of all thermocouplos woro placed in **psns** surrounded by an ico-and-water bath to kccp them at constant temperaturo. The loads to the cold-junction box are shown in figure 9. The **box** containing the ice-and-water bath is concealed! by the felt wrapping used to insulate the bath **from** the cockpit temperatures. The **switch** speed **was** such that each temperature was recorded about once every 45 seconds,

All cglinder-head and barrel temperatures were **measured**, the heads by means of gasket-type thermocouples under the rear spark plugs, and the barrels by means of thermocouples peened into the flanges at the rear center line. Other temperature recordings included.:

Intake mixture at intake ports of cylinders 5 and 10

Front and rear spark-plug elbows of cylinders 1, 7, and **11**

Right and left magnetos

Fuel cn suction **and** pressure sides of pump and in carburetor float chamber

Mixture at supercharger blower **rim**

Oil out

Oil-in line

Free air (under left wing outside slipstream, see figs. 10 and 11)

Air just ahead of screen in carburetor scoop

Air at entrance to engine compartment

Engine cooling air ahead of cylinder 1 and between cylinders 2 and 14

Engine cooling air 2 inches behind cylinder 1 and three fin spaces above bottom of head

Air at exit from oil cooler

Accessory compartment

Pilot's cockpit

Recording instrument compartment

An additional thermocouple was placed in a thermos bottle (fig. 12) containing hot ethylene glycol, the temperature of which was checked with a mercury thermometer just before take-off and just after landing.

Engine cooling, carburetor and oil-cooler air flow, as well as several additional pressure measurements, were made by means of an NACA multiple recording manometer in conjunction with twelve 9-position rotating pressure switches, which made possible the recording of 108 different pressures within about 30 seconds. The installation of the manometer and switches is shown in figures 13 and 14.

For the measurement of engine cooling-air flow, three pressure rakes were set 120° apart in the annular entrance to the engine compartment. Each rake consisted of five impact tubes spaced radially across the opening and one static tube about 1 inch to the side of the center impact tube, Figure 15 shows the right and left rakes.

The pressure at the entrance to the cylinder baffles was measured by a total of 57 impact tubes distributed.

between cylinders 1, 3, 4, 6, 7, 9, 10, 12, and 14. Each of these cylinders carried two impact tubes on the exhaust side of the cylinder, one about three fin spaces below and the other about three fin spaces above the bottom of the head; a third tube **was** in the fins on top of the cylinder head. In addition, cylinders 1, 6, and 10 had impact tubes similarly located on the intake sides of the heads and barrels and cylinders 3 and 4 carried tubes between the topmost concentric head fins and between the lowest barrel fins on the exhaust sides of the cylinders. Some of the tubes in the baffles of cylinders 9 and 10 are indicated by arrows in figure 16. The pressure rake shown was installed after completion of the tests reported herein and preparatory to tests of a blower-cooled installation. Static pressure behind the engine cylinders was measured **by** open-end tubes sheltered from direct air flow behind and just below each of the nine cylinders on which the impact tubes were placed.

The **sir flow** and the ram to the carburetor were determined by means of a rake (see fig. 17) of five impact tubes on the vertical center line of the scoop about 2 inches behind the center line of the rear cylinders and three static tubes about 1 inch to the side of the impact tubes. Holes flush with the top and bottom walls of the duct gave the static pressure in the 'boundary layer. Connections were also made to the carburetor impact-pressure tubes **below** the screen and to the pressure in the float chamber, beyond 'the altitude compensator,

Pressures in **front** of the oil cooler (fig. 18) were measured by means of three impact and three static tubes disposed along the vertical center line of the oil cooler, their openings being about 3/4 inches in front of the face of the oil cooler. Three impact tubes were placed about $\frac{1}{2}$ inch behind the rear face of *the* oil cooler, **also** on the vertical center line, and a shielded impact tube accurate to about 20° of **yaw** was set in the exit air stream at the trailing edge of the oil-cooler flap (fig. 19). The relative locations of points of pressure measurement are indicated in figures 6 and 20.

Additional pressure measurements include accessory-compartment, recording-instrument-compartment, and pilot's-cockpit pressures, as well as free-stream impact pressure.

All impact and static tubes to the manometer were of

$\frac{1}{8}$-inch copper tubing, 0.06-inch inside diameter, with leads not less than 12 nor more than 15 feet long.

Instrument readings made by the pilot included oil-in, carburetor-mixture, and free-air temperatures from vapor-pressure thermometers already installed in the airplane. For the last two flights, a resistance-bulb thermometer with a ratio-type indicator was installed in place of the vapor-pressure free-air thermonater. All free-air thermometers were calibrated for the heating effect due to speed by flying at constant altitude at several airspeeds. The calibrations are shown in figure 21. It was decided that the free-air tcmperstures recorded by the thermocouple were the most reliable, and those free-air temperatures, corroctod for compressibility, are used in this report,

Attempts were made to measure the fuel flow to the engine by two scparato methods. One method was by the use of sa BACA recording flowmeter installed in tho fuel line between the pump and tho carburetor; the other was by measuring tho pressure drops across tho main and economizer jets in the carburetor, which had boon calibrated previously on tho flow bonch. Analysis of the data subsequent to the tests indicated. that neither method gave satisfactory results as installed, and no fuel-flow data are presented in this raport. It is. thought;, however, that further development will result in making one or both of those methods of fuel-flow measurement satisfactory and may permit reclamation of the data obtained in these tests.

TEST PROCEDURE

Because the cowling was equipped with only enough cowl-flap area to cool the engine in a medium climb, all full-power testing was confined to the high-speed level-flight condition. The flight tests, then, fell into three groups: first, preliminary ground, tests and flights at increasing altitudes and powers to make sure that cooling at full powor and critical altitude would be within the allowable limits and to calibrate the airspeed head and free-air thermometer; second, full-power level flights with the original cuffs at several altitudes at and above the engine critical altitude (flights 3-6, 3-8, snd 3-9); and third, full-power lovol flights at approximately the sane altitudes as in the second group, but with tho cuff angles reduced by about 2° (flights 3-10 snd 3-11).

The typical procedure used for testing high speed and cooling pressures may be seen from an inspection of the time histories of the flights (figs. 22, 23, and 24). The pilot made a gentle climb to approximately the rated critical altitude of the engine (14,500 ft), then leveled out, closed the cowl flaps, and went to full throttle at 2700 rpm in the automatic-rich carburetor setting. After reaching constant speed, the pilot switched on the manometer and fuel flowmeter for about 40 seconds, or for slightly more than one cycle of the rotating pressure switches. (All other recording instruments were left on from take-off to landing.) The interval thus coverer?.was considered to be the "run" for purposes of determining the high-speed and cooling characteristics of the airplane at that altitude and power. Upon completion of the run, the pilot would climb to the next altitude (usually about 800 ft higher? and make another run of the same type. In each of the flights for high speed, runs were made at four altitudes. For the last flight with the modified cuffs, one high-speed run was made at an indicated altitude of 17,000 feet in automatic rich, after which the carburetor-mixture control was chnnged to full rich and then leaned out progressively in order to find whether a higher power could be attained with a different mixture. When the mixture was changed from automatic rich to full rich, the torque dropped 13 percent at constrnt engine speed; when the mixture was leaned, ths torque rose but started to fall off again after almost reaching the value obtained in the automatic rich setting. As it was not considered safe to lean the mixtures below the point at which the torque started to fall off, the pilot immediately set the mixture control back to automatic rich and ended the experiment. A subsequent study of the relative fuel-flow data indicated, however, that the rate of fuel flow to the engine during manual mixture control was never as low as the rate of fuel flow in automatic rich, the unexplored region was indicated to be of the order of 70 pounds of gasoline per hour. The fuel-flow records also indicated that the mixture was becoming slightly richer, rather than leaner, during the last part of the period of manual control.

RESULTS

In figures 22, 23, and 24 are presented time histories of the main high-speed flights, giving the recorded pressure altitude; indicated airspeed; manifold pressure;

torque; engine speed; and head, barrel, and other selected temperstures during the flight. The brake horsepower as calculated from the torque and Engine-speed curves is also given.

The periods of steady level flight at different altitudes during which the high speed was being measured are indicated on the time histories. The data pertinent to the determination of' maximum speed that were recorded during these runs are plotted to an enlarged scale in figure 25. The values of maximum speed and power calculated from these data for each run are given in table I along with simultaneously recorded data on engine temperatures and cooling and induction air pressures.

DISCUSSIOB

Maximum Speed

The values of maximum speed given for each run in table I were computed from values of impact and static pressure selected, after inspection of the enlarged time histories of figure 25, as being most representative of steady level flight. Comparison of the values for all runs over the altitude range covered shows a maximum spread of approximately 5 miles per hour in speed. The faired curve of speed against altitude in figure 2% suggests that about 20 percent of this spread is attributable to a consistent variation of speed with altitude. The remaining spread of approximately 4 miles per hour indicates the consistency with which the maximum speed values could be reproduced in different runs under different atmospheric conditions.

The relation between the observed variations of power and speed with altitude shown in figure 26 is most easily understood by consideration of the equilibrium of power required and power available in steady level flight. Under these conditions

$$\frac{DV}{375} = \eta \ bhp \qquad (1)$$

or

$$V = 52.73 \left(\frac{\eta}{SC_D}\right)^{1/3} \left(\frac{bhp}{\sigma}\right)^{1/3} \qquad (2)$$

where

D   over-all brag of airplane, pounds

V   true airspeed, miles per hour

η propulsive efficiency of propeller and exhaust
            stack combination

bhp   brake horsepower

S   wing area, square feet

C_D drag coefficient of airplane

σ density ratio

It is immediately apparent; that, for full-throttle
level flight at and slightly above the critical altitude
of an airplane of normal aspect ratio and wing loading
and a propeller chosen for good high-speed performance,

the value of the parameter $52.73 \left(\dfrac{\eta}{SC_D} \right)^{1/3}$ should be vir-

tually unaffected by moderate changes in weight or alti-
tude. Values of this parameter deduced from the observed

values of V and $\dfrac{bhp}{\sigma}$ for each run are plotted against

density altitude in figure 27. As expected, little varia-
tion with altitude is apparent.

Under the conditions just described, the parameter

$\left(\dfrac{bhp}{\sigma} \right)^{1/3}$ would also be expected to remain essentially con-

stant over the altitude range covered by the tests. The
measured values of this parameter, which are also plotted
against density altitude in figure 27, confirm this expec-
tation.

One important phase of the present investigation in-
volves comparison of the high-speed performance of the
short-nose cowling and exhaust stack arrangement with that
of a similar long-nose version tested previously on the
same airplane (reference 4). It has also been suggested
that the results might be compared with accepted high-
speed performance results for similar airplanes with con-
ventional air-cooled (P-36A) and liquid-cooled (P-40C) in-

stallations. In order to provide such a comparison, equation (2) in the modified form

$$\left(\frac{V}{52.73}\right)^3 = \left(\frac{\eta}{SC_D}\right)\left(\frac{bhp}{\sigma}\right) \qquad (3)$$

is presented graphically in figure 28. Points representing the high-speed performance of the various airplanes, all of which have the same wing area, are spotted in this figure. The location of a point on the figure immediately reveals not only the maximum speed of the airplane but also the manner by which that speed is attained; that is, by power, supercharging, and ram as indicated by the ordinate scale, or by aerodynamic refinement, as indicated by the abscissa scale.

Within reasonable limits, the figure may be used for several purposes. Primarily, it provides a ready method for determining the effect on maximum speed of changing the critical altitude of an engine installation by either supercharging or ram, or by reducing preheating of the ` carburetor air. When the corresponding Changes in the weight and the propulsive efficiency are small, the effect on the factor $\frac{\eta}{SC_D}$ will be negligible. The abscissa of a point on the figure may therefore be assumed to remain constant while the ordinate is shifted. For instance, for purposes of comparing the cleanness of the two installations in terms of speed at the same horsepower and altitude, it might be assumed that the induction system of the long-nose XP-42 could be modified without increase in drag to get the same high ram as obtained with the short-nose XP-42. In that case, as the same engine was used in both installations, the observed points for the long nose would be shifted upward to the same average value of $\frac{bhp}{\sigma}$ as was observed for the short nose; and the long-nose installation would be expected to attain a maximum speed of 341 miles per hour, compared with the observed maximum speeds of 336 miles per hour for the short nose and 338 miles per hour for the long nose. The chart shows then that the cleanness of the long-nose installation is not fully exploited because of losses in the induction system.

The comparison may be extended to include the E-36A and P-40C, with limitations to be noted later. Inasmuch as the engines of all these airplanes have been rated at

Airplane	Observed maximum speed (mph)	Maximum speed at 1050 hp at 15,000 ft (mph)
XP-42 long nose X		352
P-36A		335

The comparison, however, does appear to indicate that, by use of individual jet exhaust stacks and a high-inlet-velocity cowling, the installation of an air-cooled engine may be made to compare favorably with a conventional liquid-cooled engine installation.

Pressures and Temperatures

The variation of cylinder temperatures around an engine is influenced by a number of factors, such as non-uniform charge and mixture distribution, that are in no way a function of the cowling design. Unless the effect of these factors can be determined, the merit of a cowling designed for general application cannot be reliably

evaluated **by** measurements of engine temperatures alone on
a specific application. **For** this reason, primary empha-
sis in the present tests has been centersd on determining
the extent to which the type of cowling under considera-
tion provides a high, uniformly distributed pressure over
the front of the engine and a suitable, uniformly distrib-
uted preesure over the rear of the engine.

Figures 29 to 31 present the results of the pressure
and temperature measurements in a graphical form that shows
tho distribution of both pressure and temperature around
the engine for several typical runs. These data indicate
that, while pressures at the **baffle** entrances vary some-
what with the location of the cylinders on which they are
measured, they vary even more critically with the point of
measurement on the individual cylinder. Values, averaged
around the engine,, **of** the front pressures recorded at par-
ticular lobations in the cylinder **baffles** are given in
table II. They indicate a deficiency of front prsssuro
at tho top of the heads of tho front cylinders and at the
bottom of the barrels of both front and rear cylinders.

In tho typo of cowling under consideration, in which
cooling ais is introduced to the engine compartment through
a fairly narrow annular opening, tho front pressures on the
engine, **and.** particularly on tho front cylinders, may be ex-
pected to vary up and down tho cylinder with respect to
the location of the entoring jet, tho magnitude of tho var-
iation dopending upon tho velocity of tho jot and tho dis-
tance of tho cylinder behind tho jot. If space permits
tho use of a well-designed diffuser section in tho annulus,
the jot ontering the ongiae compartment will have negligi-
ble velocity head and turbulent losses will also bo negli-
gible. The result should then bo a high uniform pressure
on tho front of tho engine, tho pressure being equal to
that in the annulus. If such a diffuser is not or cannot
bo used, it may reasonably bo expected that the maximum
variation of front prcssuros will not exceed tho differ-
ence botween tho impact pressure and static pressure of
the **air** at tho exit **from** tho diffuser, or, tho velocity
head of tho jot. It is interesting to note in this **con-**
nection that the lowest pressures measured in the baffles
were approximately equal to tho measured static pressure
In tho annulus and that none of tho front prsssurcs were
as high as the impact pressure in the annulus. Tho aver-
age pressure on tho front of tho engine was approximately
$0.12q_c$ lower than tho average impact pressure in the annu-
lus (q_c, airplane impact press.),

The general trend of **pressure** distribution around the engine indicates that the highest front pressures occurred on the bottom of the engine; whereas the lowest front pressures occurred on the right and the left upper sides of the engine. When average pressures over all high-speed runs are plotted **for** each common point of pressure measurement, as in figure **32, it** is seen that the only points following this trend are the pressures on top of the heads. With the exception of cylinder 3, the distribution of pressure on the side of the heads and barrels was uniform around the engine. The pressure tubes on the side of cylinder 3 were directly behind a large ignition-cable conduit and probably lay in its wake. Although there were usually other obstructions, such as push **rods** and **ignition** cables, in front of the other **pressure** tubes, none were so large as the conduit. These obstructions, however, may account for some of the observed difference in total pressure between the annulus and the engine,

Individual cylinder temperatures **showed** little tendency to correlate with the pressure drops across the individual cylinders. It may be noted in particular that, although pressures over the top of the front cylinder heads were lower than those over the top of the rear heads, the front head temperatures were lower than those of the rear heads. In this case, the observed pressures on top of the front heads may provide erroneous indications of the air flow, because the tops of the fins, where the pressure tubes were located., were above the direct air jet But the Lower halves of the fins were exposed to the jet from the annulus. (See fig. 6.)

An inspection of the cylinder temperatures around the engine shows that the right side of the engine was cooler than the left. The left cylinder heads were on the average, about 35° F hotter than the right, and the left cylinder bases were correspondingly about 10° F hotter than the right. The front base temperatures were slightly higher than the resr base temperatures. There is no apparent explanation why the left side of the engine was hotter thnn the right, because front and rear cooling-air pressures were nearly uniform.

In figure 33 average head and barrel temperstures in $^{\circ}F$ above free-air temperature are plotted, along with the cooling-air pressure drops, averaged over the ongine, for full-throttle operation over a range of density altitudes above the critical. Also shown are tho brake horsepower

and manifold. pressure. The change from the original cuffs (flights 3-8 and 3-9) to the modified cuffs (flight 3-10) produced. little apparent change in any of the quantities shown. Although individual pressures **and** temperatures showed little correlation, the variation of average pressures **and** temperatures was consistent.

A considerable rise in cylinder temperatures at altitudes above critical altitude appears to have resulted from the net effect of decreasing power and decreasing pressure drop. An important probable factor in this temperature rise, however, was the decrease in fuel-air ratio as the manifold pressure decreased at altitudes above the critical altitude. The power compensation of this carburetor depends upon the manifold **pressure.**

The recommended limiting temperatures for the engine used in those tests were 500 F for the cylinder heads and 335° F for the barrels at the points of measurement used. Army specifications require that the installation be capable of operating within these limiting temperatures under "summer conditions," that is, sea-level temperature is 100° F and the variation of temperature with pressure altitude is 3.6° F per 1000 feet. For correcting tests to those air conditions, a 1:1 temperature correction factor is specified for both heads and barrels. Figure 34 **shows** the observed head and barrel temperatures in relation to those Army limits. It is immediately apparent that, **although** head temperatures were relatively **low,** the maximum barrel temperatures exceeded the Army limits at and above critical altitude even though the engine was operating below its rated military power. A radistribution of available cooling air to provide more pressure at the base of the cylinders **would** probably correct this condition.*

Figure 35 presents a comparison of the average pressures available at several locations in the cowling. The highest pressures were observed in the carburetor duct,

_____

Subsequent tests on the same engine and thermocouple installation in another short-nose cowling showed that a reduction of 15° F in the temperature of the base thermocouples could be obtained by removal of the baffle sealing strips between the barrels at the bottom of the cylinders. The sealing strips are a special feature of the particular baffle arrangement provided by Pratt & Whitney Aircraft for the engine used in this investigation and are not present in the standard baffle installation for 1830 engines.

where the average pressure was about 104 percent of free-stream impact pressure. This result indicated that the cuffs were loaded even in the high-speed condition. The difference in average pressure between the carburetor duct and the annulus is largely chargeable to the boundary-layer effect on the spinner; whereas the difference between the annulus and the front of the engine, as has been noted, was probably caused by turbulent losses in the rapid expansion from the annulus to the engine compartment. The large boundary-layer effect on the inner edge of the annulus, which forms a continuation of the spinner, may be observed in figure 36, which shows the average pressure distribution in the annulus and in the carburetor duct. The data in table I on impact and static pressures at the surveys in the annular entrance to the engine compartment indicate that the ratio of the velocity head at any point in the survey plane to free-stream impact pressure remained essentially constant over the range of power, altitude, and angle-of-attack conditions covered during the full-throttle high-speed runs. From the faired curves of the ratio of impact and static pressures to free-stream impact pressure, averaged for all three surveys and all high-speed runs as shown in figure 36, it has been found that

$$\int_{\text{inner wall}}^{\text{outer wall}} \sqrt{\frac{\frac{1}{2}\rho_s V_s^{\,2}}{q_c}}\ dA = 0.640$$

where

$\dfrac{1}{2}\rho_s V_s^{\,2}$ dynamic pressure at surveys, pounds per square foot

q_c airplane impact pressure, pounds per square foot

A area of annular entrance at survey, square feet

ρ_s air density at survey plane, slugs per cubic foot

V_s air velocity at survey plane, feet per second

The mass flow of air to the engine is

$$\rho_s V_s A = 0.640 \sqrt{2\rho_s q_c}$$

The volume **flow** of free air at density ρ_{fa} is

$$\frac{\rho_s V_s A}{\rho_{fa}} = 0.640 \sqrt{\frac{2\rho_s q_c}{\rho_{fa}^2}}$$

Temperature and pressure measurements at the surveys indicate that the density at the surveys ranged- from **4** to 6 percent above free-ais density so that

$$\text{Volume flow} = 0.928 \sqrt{\frac{q_c}{\rho_{fa}}}$$

Inspection of figure 35 shows that, within the limits of experimental error, the value of $\sqrt{\dfrac{q_c}{\rho_{fa}}}$ ay be taken as 357 at all altitudes covered by the tests. Hence, the flow of cooling air to the engine was 331 cubic feet of free air per second, or 19,860 cubic feet of free air per minute.

Evaluated in a similar nanncr, the data. for the **flow** in the carburetor duct indicates that

$$\text{Volume flow} = 0.138 \sqrt{\frac{q_c}{\rho_{fa}}} \quad \text{cubic feet per second}$$

$$= 2960 \text{ cubic feet of free air per minute}$$

Inasmuch **as** the ratio of horsepower to density was constant, this result lcads to the conclusion that tho specific air consumption was **also** nearly constant at 8.9 pounds por brake horsopowor-hour.

CONCLUSIONS

Results have boon givan of high-speed lovel-flight tests of a short-noso high-inlet-velocity cowling with propellor cuffs on the XP-42 airplano. These results are intonded for use in comparisons with other cowlings tested on the same airplano, and for this roason the data obtained have boon fully prosontod.

1. The observed airplane aaximum speed was 336 milos per hour at 960 horsepower at 15,000 fcot density altitude.

2. Cooling-ais prossurs recovery on tho front of the engine averaged about 80 percent of free-stream impact pressure. The pressure distribution was fairly uniform.

3. With 15 inches of water pressure drop across the engine, the cylinder head temperatures were relatively low, but cylinder base temperatures were slightly above their Army limit.

Langley Memorial Aeronautical. Laboratory,
   National Advisory Ccmmittee for Aeronautics,
      Langley Field, Va.

REFERENCES

1. Valentine, E. Floyd: Preliminary Investigation Directed toward Improvement of the NACA Cowling. WACA A.R.R., April 1942.

2, Silverstein, Abe, and Guryansky, Eugene R.: Development of Cowling for Long-Bose Air-Cooled Engine in the NACA Full-scale Wind Tunnel, NACA A.R.R., Oct. 1941.

3. Pinkel, Benjamin, Turner, L. Richard, and Voss, Fred: Design of Nozzles for the Individual Cylinder Exhaust Jet-Propulsion System. NACA A.C.R., April 1941.

4. Bailey, F. J., Jr,, Johnston, J. Ford, and Voglewede, T. J.: Flight Investigation of the Performance and Cooling Characteristics of a Long-Nose High-Inlet-Velocity Cowling on the XP-42 Airplane. NACk A.R.R., April 1942.

TABLE Ia.-PRESSURE AND TEMPERATURE DATA

Flight			3-6			3-8				3-9				3-10				3-11
Run			2	3	4	1	2	3	4	1	2	3	4	1	2	3	4	1
True airspeed, mph			337	334	333	338	334	336	336	335	335	333	333	336	335	336	335	337
Density altitude, ft			16850	17000	17800	14900	15800	16550	17300	14950	16000	17050	18300	15250	16000	17100	18050	18000
Atm press., in. Hg			16.71	16.26	15.74	17.30	16.71	16.16	15.65	17.37	16.58	15.94	1525	17.26	16.56	15.92	15.26	15.28
Ambient air temp, °F			21	19	16	15	13	9	5	18	12	10	8	19	13	10	5	5
Ground air temp, °F			69	69	69	62	62	62	62	78	78	78	78	62	62	62	62	63
σ, density ratio			.602	.588	.573	.631	.612	.598	.584	.630	.609	.588	565	.624	.607	587	569	.570
rpm			—			2680	2680	2680	2680	2680	2680	2680	2680	2700	2700	2700	2700	2700
bhp			924	905	882	960	933	912	886	956	933	900	872	947	920	884	855	867
Manifold press., in. Hg			—	—	—	41.2	39.7	38.6	37.6	41.1	39.5	36.0	36.4	41.1	39.7	38.1	36.8	36.8
q_c, Impact press. in. H₂O			35.4	34.0	33.0	37.8	35.6	34.9	34.2	36.6	35.4	33.7	32.5	36.5	35.4	34.4	33.	33.5
Pressure ratio $\frac{p}{q_c}$																		
Engine pressure tube locations	1-R	Sheltered tubes behind engine	.39	.40	.42	.41	42	41	.40	40	38	39	39	39	39	39	39	39
	3-R		.39	.40	.42	.41	.42	.41	40	.40	38	34	39	39	39	39	39	
	4-R		37	38	40	.39	40	40	.39	38	36	38	38	38	38	37	37	
	6-R		39	.39	41	41	42	41	40	40	.38	39	39	39	40	39	39	
	7-R		"	40	42						"	"	"	"	39	"	34	
	9-R		"	"		"	"	"	"	"	"	"		"	40	"	40	40
	10-R		"	"	"	"	"			"	"		"	"			39	40
	12-R		"	"	"	"					"	"						39
	14-R			"	"	"	"							"	.39			.39
	1-TH	Top of head	76	77	80	78	78	77	77	78	75	77	76	79	77	80	77	76
	3-TH		79	81	83	80	81	81	81	81	7P	80	80	80	81	81	81	80
	4-TH		70	72	73	72	73	72	72	72	70	71	72	70	71	70	71	70
	6-TH		72	72	74	73	74	73	74	73	71	72	72	72	73	72	73	72
	7-TH		81	82	84	82	83	76	76	.83	.81	80	81	80	81	81	81	80
	9-TH		82	84	85	83	84	84	.84	.83	81	83	83	82	83	83	83	83
	10-TH		76	.75	78	75	77	76	75	75	74	75	75	74	75	74	75	75
	12-TH		73	74	75	73	75	74	73	73	72	73	72	72	73	72	73	73
	14-TH		.69	.71	.73	.71	.72	.71	.71	.71	.69	71	.70	69	.70	70	70	71
	1-EH	Exhaust side of head	.86	86	89	E6	87	87	86	86	86	86	86	-	-			
	3-EH		78	78	.81	79	79	78	78	79	77	77	78	77	77	77	77	77
	4-EH		88	.89	90	89	90	.89	89	90	82	89	88	88	89	88	85	88
	6-EH		.81	83	85	.84	.83	83	83	.83	.80	82	83	81	81	81	81	82
	7-EH		84	.86	a9	.86	87	a7	87	86	.86	85	85	85	85	84	85	86
	9-EH		86	87	89	.85	86	85	85	.84	84	84	84	84	85	84	84	84
	10-EH		86	88	90	.87	88	87	87	.87	.86	86	87	.86	87	87	86	87
	12-EH		86	87	89	88	E8	87	.87	.86	.85	85	85	84	84	83	84	84
	14-EH		.83	.84	85	.84	85	.84	83	.84	.82	83	83	E2	.83	.82	82	83
	1-EB	Exhaust side of barrel	.84	85	87	85	85	84	84	84	83	83	83	84	84	83	83	85
	3-EB		.68	70	72	70	71	70	70	70	69	69	70	69	70	69	69	—
	4-EB		78	74	.80	79	80	79	.79	.80	78	79	79	79	80	79	79	79
	6-EB		.81	E3	85	83	83	.83	.83	.83	.80	82	.82	.82	a3	.82	83	83
	7-EB		.80	81	83	81	81	81	.81	.82	.80	81	81	79	80	80	80	80
	9-EB		.82	.83	86	83	84	83	84	.83	82	82	.83	.82	83	82	83	83
	10-EB		77	77	80	78	80	79	79	.78	77	77	77	80	78	77	78	77
	12-EB		78	.80	82	80	80	80	.80	79	78	79	78	79	80	78	79	79
	14-EB		78	.80	82	.80	.80	.80	80	.79	.78	.79	.78	.78	.80	78	79	74
	1-IH	Intake side of head	82	E2	84	82	84	82	62	81	81	81	82	81	81	81	82	82
	6-IH		.87	.88	90	.89	90	.88	.89	.89	86	85	88	88	88	88	88	.89
	10-IH		89	91	93	91	93	91	.92	90	89	90	90	91	92	91	91	91
	1-IB	Intake side of barrel	77	78	81	79	78	78	78	78	77	78	77	78	77	76	77	78
	6-IB		.85	86	88	.86	.87	86	85	86	85	85	85	85	85	85	85	86
	10-IB		.82	82	.85	.83	83	82	.82	.83	82	82	82	83	82	81	82	.84
	3-EH2		78	.80	82	.80	80	79	80	.80	78	79	80	79	81	80	80	79
	4-EH2		.86	.86	.87	.88	.89	.88	87	.89	86	86	E7	85	86	84	85	86
	3-EB2		.64	.66	67	.66	.67	.66	66	65	64-	68	65	64	65	64	64	65
	4-EB2		.67	.69	.70	.68	.69	.68	.68	.66	66	.67	66	69	.70	.67	.71	69

cylinder

Method of designating tube locations for typical cylinders

Cylinder 1.
1-TH
1-IH
1-EH
1-IB
1-EB
1-R

Cylinder 3.
3-TH
3-EH2
3-EH
3-EB
3-EB2
3-R

TABLE Ib.- PRESSURE AND TEMPERATURE DATA
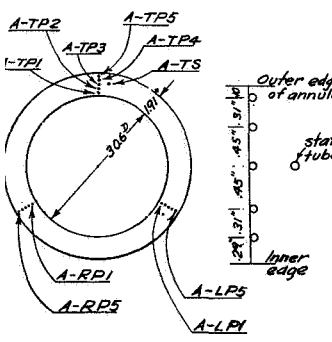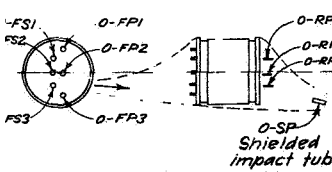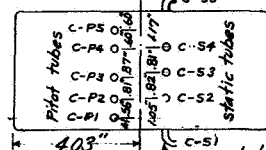
	Flight	3-6			3-8				3-9				3-10				3-11
	Run	2	3	4	1	2	3	4	1	2	3	4	1	2	3	4	1
	True air speed, mph	337	334	333	338	334	336	336	335	335	333	333	336	335	336	335	337
	Density altitude, ft	16350	17100	17800	14900	15800	16550	17300	14950	16000	17050	18300	15250	16000	17100	18050	18000
	Atm. press., in Hg	16.71	16.26	15.74	17.30	16.71	16.16	15.65	17.37	16.58	15.94	15.25	17.26	16.56	15.92	15.26	15.28
	Ambient air temp, °F	21	19	16	15	13	9	5	18	12	10	8	19	13	10	5	5
	Ground air temp, °F	69	69	69	62	62	62	62	78	78	78	78	62	62	62	62	63
	σ, density ratio	.602	.588	.573	.631	.612	.598	.584	.630	.609	.588	.565	.624	.607	.587	.569	.570
	rpm	2680	2680	2680	2680	2680	2680	2680	2680	2680	2680	2680	2700	2700	2700	2700	2700
	bhp	924	905	882	960	933	912	886	956	933	900	872	947	920	884	855	867
	Manifold press, in.Hg	—	—	—	41.2	39.7	38.6	37.6	41.1	39.5	38.0	36.9	41.1	39.7	38.1	36.8	36.8
	q_c, impact press in. H_2O	35.4	34.0	33.0	37.3	35.6	34.9	34.2	36.6	35.9	33.7	32.5	36.5	35.9	34.4	33.1	33.5

Pressure ratio, p/q_c

Annulus pressure tube locations			2	3	4	1	2	3	4	1	2	3	4	1	2	3	4	1
	A - TP1	Top survey Impact tubes	.84	.86	.88	.85	.86	.85	.85	.85	.84	.84	.84	.85	.86	.85	.85	.86
	A - TP2		.92	.95	.90	.94	.95	.94	.93	.93	.93	.93	.93	—	—	—	—	.93
	A - TP3		.94	.97	.98	.97	.98	.95	.94	.96	.94	.96	.95	.95	.97	.95	.96	.96
	A - TP4		.95	.97	.98	.98	.96	.97	.97	.97	.95	.96	.95	.95	.96	.95	.97	.97
	A - TP5		.90	.94	.98	.91	.92	.90	.90	.93	.92	.92	.92	.90	.91	.90	.90	.90
	A - TS	Static tube	.66	.66	.68	.68	.68	.67	.67	.67	.66	.66	.67	.66	.67	.66	.67	.67
	A RP1	Right survey impact tubes	.84	.86	.88	.84	.86	.85	.84	.85	.83	.83	.84	.83	.83	.83	.84	.82
	A RP2		.92	.95	.90	.94	.95	.95	.94	.95	.94	.94	.94	.93	.94	.93	.95	.93
	A RP3		.97	.98	1.00	.99	1.00	.98	.98	.99	.97	.98	.99	.96	.97	.97	.97	.97
	A RP4		.97	.97	.99	.97	.98	.97	.97	.99	.97	.97	.97	.95	.96	.95	.96	.96
	A RP5		.89	.90	.92	.90	.90	.89	.88	.90	.89	.89	.88	.88	.89	.88	.88	.88
	A - RS	Static tube	.66	.66	.68	.68	.68	.67	.67	.67	.66	.67	.67	.66	.67	.66	.67	.67
	A - LP1	Left survey impact tubes	.86	.88	.89	.87	.87	.86	.86	.85	.86	.86	.84	.86	.86	.85	.86	.87
	A - LP2		.94	.96	.91	.96	.95	.95	.94	.96	.94	.95	.95	.96	.95	.94	.96	.95
	A - LP3		.98	.99	1.01	1.00	1.00	.99	.99	.99	.97	.99	.99	.96	.97	.97	.97	.98
	A - LP4		.97	.97	1.00	.98	.99	.98	.98	.96	.97	.97	.97	.98	.99	.98	.98	.98
	A - LP5		.86	.87	.89	.87	.87	.86	.87	.87	.85	.85	.86	.87	.88	.86	.87	.87
	A - LS	Static tube	.72	.73	.75	.73	.74	.73	.73	.74	.72	.73	.73	.71	.72	.71	.72	.73
Oil cooler pressure tube locations	O - FP1	Front survey impact tubes	1.01	1.01	1.04	.99	.99	.98	.99	.99	.97	.97	.99	.96	.97	.98	.97	1.01
	O - FP2		1.04	1.04	1.06	1.03	1.03	1.03	1.03	1.03	1.02	1.08	1.03	1.02	1.00	.97	1.03	1.04
	O - FP3		1.04	1.05	1.06	1.05	1.05	1.05	1.05	1.05	1.04	1.04	1.05	1.04	1.03	—	—	1.05
	O - FS1	Static tubes	.91	.92	.93	.93	.93	.92	.92	.92	.90	.91	.92	.90	.91	.92	.91	.93
	O - FS2		.92	.93	.94	.93	.93	.92	.94	.94	.91	.92	.93	.91	.91	.92	.92	.93
	O - FS3		.94	.94	.96	.94	.94	.94	.95	.94	.94	.93	.94	.92	.93	.93	.94	.96
	O - RP1	Rear survey impact tubes	.71	.71	.73	.71	.72	.71	.71	.72	.69	.71	.71	.70	.71	.69	.70	.72
	O - RP2		.81	.83	.85	.83	.83	.83	.82	.83	.80	.83	.82	.81	.81	.81	.82	.83
	O - RP3		.59	.61	.63	.60	.61	.60	.60	.59	.58	.59	.60	.58	.59	.59	.60	.62
	O - SP	Shielded impact tube	.59	.60	.62	.60	.60	.60	.59	.59	.57	.58	.59	.58	.59	.58	.59	.60
Carburetor scoop pressure tube locations	C - P1	Impact tubes	1.02	1.02	1.04	1.03	1.04	1.02	1.03	1.03	1.02	1.01	1.02	1.01	1.01	1.01	1.01	1.01
	C - P2		1.03	1.04	1.06	1.03	1.04	1.03	1.04	1.05	1.04	1.03	1.03	1.02	1.02	1.02	1.02	1.02
	C - P3		1.04	1.06	1.07	1.05	1.06	1.04	1.05	1.05	1.04	1.04	1.05	1.03	1.05	1.04	1.03	1.04
	C - P4		1.05	1.07	1.09	1.07	1.07	1.06	1.06	1.07	1.05	1.05	1.05	1.04	1.05	1.04	1.04	1.04
	C - P5		1.06	1.07	1.09	1.07	1.07	1.06	1.06	1.07	1.05	1.06	1.06	1.04	1.05	1.05	1.05	1.04
	C - S1	Static tubes	.86	.86	.88	.86	.87	.87	.86	.86	.85	.86	.86	.85	.85	.84	.84	.86
	C - S2		.84	.84	.86	.84	.85	.84	.84	.84	.84	.84	.84	.82	.83	.83	.83	.83
	C - S3		.83	.84	.87	.84	.84	.84	.84	.84	.82	.83	.84	—	—	—	—	—
	C - S4		.84	.84	.87	.84	.85	.84	.84	.85	.83	.84	.84	.82	.83	.82	.83	.84
	C - S5		.84	.85	.87	.84	.85	.84	.85	.85	.84	.84	.84	.83	.83	.83	.83	.84

TABLE Ic.-PRESSURE AND TEMPERATURE. DATA

Test - Flight	3-6			3-8				3-9				3-10				3-11
Run	2	3	4	1	2	3	4	1	2	3	4	1	2	3	4	1
True airspeed, mph	337	334	333	338	334	336	336	335	335	333	333	336	335	336	335	337
Density altitude, ft	16350	17000	17800	14900	15800	16550	17300	15950	16000	17050	18300	15250	16000	17100	18050	18000
Atm press, in. Hg	16.71	16.26	15.74	17.30	16.71	16.16	15.65	17.37	16.58	15.94	15.25	17.26	16.56	15.92	15.26	15.28
Ambient air temp, °F	21	19	16	15	13	9	5	18	12	10	8	19	13	10	5	5
Ground air temp, °F	69	69	69	62	62	62	62	78	78	78	78	62	62	62	62	63
σ, density ratio	.602	.588	.573	.631	.612	.598	.584	.630	.609	.588	.565	.624	.607	.587	.569	.570
rpm	2680	2680	2680	2680	2680	2680	2680	2680	2680	2680	2680	2700	2700	2700	2700	2700
bhp	924	905	882	960	933	912	886	956	933	900	872	947	920	884	855	867
Manifold press, in.Hg	—	—	—	41.2	39.7	38.6	37.6	41.1	39.5	38.0	36.4	41.1	39.7	38.1	36.8	36.8
q_c, impact press. in. H_2O	35.4	34.0	33.0	37.3	35.6	34.9	34.2	36.6	35.4	33.7	32.5	36.5	35.4	34.9	33.1	33.5

Cylinder—point of measurement — Temperature °F

gasket thermocouple at rear sparkplug

Cyl	3-6 2	3-6 3	3-6 4	3-8 1	3-8 2	3-8 3	3-8 4	3-9 1	3-9 2	3-9 3	3-9 4	3-10 1	3-10 2	3-10 3	3-10 4	3-11 1
1	392	342	403	388	388	390	403	37D	370	379			382	384	393	398	396
2	405	390	403	399	—	397	410	385	385	388		.395	392	395	400	400
3	392	392	399	396	388	390	397	.374	374	379		384	38C	388	391	391
4	thermocouple broken			thermocouple broken												
5	367	369	392	.365	365	369	376	360	363	367		.366	362	366	369	370
6	430	428	435	421	424	424	430	417	419	419		418	422	425	429	425
7	383	381	390	381	379	387	387	365	372	370		373	375	378	382	386
8	415	419	424	406	408	408	419	397	403	403		405	407	407	407	406
9	421	428	432	414	415	421	428	410	412	415		418	418	422	422	41.
'0	428	430	437	424	423	428	433	415	415	417		418	422	423	429	422
2	403	405	414	349	399	405	412	394	394	397		400	400	405	405	406
3	424	428	435	419	421	424	433	412	415	417		420	422	424	431	431
4	423	424	432	414	415	419	428	405	405	410			414	418	423	422

rear ℄ of flange at base of cylinder — thermocouple broken

Cyl	3-6 2	3-6 3	3-6 4	3-8 1	3-8 2	3-8 3	3-8 4	3-9 1	3-9 2	3-9 3	3-9 4	3-10 1	3-10 2	3-10 3	3-10 4	3-11 1
?	311	309	311	302	302	302	311	297	297	300		301	303	307	308	308
3	300	300	302	293	293	295	300	288	286	288		294	296	296	298	299
t	302	302	304	295	293	295	300	286	286	288		293	298	299	298	296
5	288	288	289	282	284	286	288	275	275	279		287	287	287	287	287
5	304	304	306	297	297	300	304	293	289	293		303	303	303	303	303
7	293	293	295	286	286	289	291	279	280	:a2		289	290	290	290	288
9	295	295	297	293	289	293	295	286	286	288		289	"90	273	290	294
9	306	311	311	302	302	302	307	295	297	300		301	303	303	303	305
0	320	325	324	316	316	318	320	309	309	311		314	316	319	319	317
1	293	297	297	286	286	288	293	286	282	288		289	290	294	290	294
?	311	320	324	309	311	313	318	304	30C	306		310	312	314	314	314
3	300	302	304	296	296	297	324	293	289	293		296	299	303	303	303
4	311	311	311	304	304	302	313	297	297	300		305	307	308	308	305

(note in 3-9 / 3-10 area: "no temperature record")

Point of measurement	3-6 2	3-6 3	3-6 4	3-8 1	3-8 2	3-8 3	3-8 4	3-9 1	3-9 2	3-9 3	3-9 4	3-10 1	3-10 2	3-10 3	3-10 4	3-11 1
0 — intake port	225	225	225	217	217	2	217	214	210	210		217	217	215	215	215
Mixture at blower rim	163	156	163	156	154	151	149	147	147	147		159	157	154	154	146
Fuel on suction side of pump	77	81	84	81	sa	86	86	77	73	77		71	71	71	78	78
" " pressure "	84	90	90	ma	86	86	86	81	77	a i		78	82	78	86	78
" at outlet of flow meter	88	93	93	86	86	90	90	84	84	84		82	83	82	87	80
in carburetor float chamber	84	88	90	86	86	82	86	77	75	75		78	78	82	82	78
- front spark plug elbow	46	46	46	68	39	39	39	68	68	68		44	47	49	49	40
- rear " "	88	84	88	81	77	77	72	72	68	68		78	78	74	71	71
7 - front	46	46	46	39	39	39	39	46	48	55		49	49	46	49	40
7 - rear	55	54	54	52	52	48	39	46	43	36		53	49	46	40	40
/ - front	50	46	46	46	46	43	39	43	39	36		49	46	4Q	37	36
/ - rear	81	81	81	77	77	77	72	68	68	68		78	78	74	71	71
Recorded free air	39	38	34	33	32	27	23	36	30	25		37	31	28	23	23
Pilot's observed free air	37	35	33	36	33	31	29	35	32	4	25	31	29	25	20	14
Air in carburetor scoop	46	46	46	46	39	39	36	39	36	30		46	42	37	33	31
at top annular rake	46	46	46	46	39	39	36	39	10	32		46	40	37	33	31
in front of cylinder 1.	54	54	50	52	48	48	43	46	59	36		49	49	46	40	40
behind cylinder 1.	183	192	190	172	169	176	167	131	-	-		—	—	—	—	—
" at exit from oil cooler	81	81	81	77	72	70	72	68	61	47		74	71	69	62	62
Oil in line	138	138	138	133	133	131	133	131	133	29		134	34	132	132	132
" out	214	214	214	208	208	207	207	203	201	201		206	206	208	204	200
Accessory compartment	126	129	129	124	120	118	122	09	06	06		119	119	116	116	110
Right magneto	thermocouple broken															
Left	108	108	108	106	106	104	102	97	13	97		107	103	103	100	90
Pilot's cockpit (recorded)	90	97	97	90	90	90	86	88	88	84		91	87	89	87	76
(observed)		—	—	90	90	90	89	86	86	85	84					79
Recording instrument compartment	88	93	93	86	86	86	84	81	81	77		87	87	85	85	74

TABLE II

AVERAGE COOLING AIR PRESSURES AT SEVERAL LOCATIONS ON FRONT AND REAR CYLINDERS

Locations	Flight	3-6			3-8				3-9				3-10				3-11
	Run	2	3	4	1	2	3	4	1	2	3	4	1	2	3	4	
					Average pressure, p/q_c												
Top of heads	Front cylinder	0.72	0.73	0.75	0.73	0.74	0.73	0.73	0.73	0.71	0.72	0.72	0.71	0.72	0.72	0.72	0.72
	Rear cylinder	.80	.81	.83	.81	.82	.80	.80	.81	.79	.80	.80	.80	.81	.81	.81	.80
Exhaust side of heads	Front cylinder	.85	.86	.88	.86	.87	.86	.86	.86	.83	.85	.85	.84	.85	.84	.84	.85
	Rear cylinder	.84	.84	.87	.84	.85	.84	.84	.84	.85	.83	.83	.82	.82	.82	.82	.82
Exhaust side of barrels	Front cylinder	.78	.80	.82	.80	.81	.80	.80	.80	.78	.79	.79	.80	.80	.79	.80	.80
	Rear cylinder	.79	.80	.82	.80	.81	.80	.80	.80	.79	.79	.79	.79	.79	.79	.79	.83
Intake side of heads	Front cylinder[1]	.88	.90	.92	.90	.92	.90	.91	.90	.88	.88	.89	.90	.90	.90	.90	.90
	Rear cylinder[2]	.82	.82	.84	.82	.84	.82	.82	.81	.81	.81	.82	.81	.81	.81	.82	.82
Intake side of barrels	Front cylinder[1]	.84	.84	.87	.85	.85	.84	.84	.85	.84	.84	.84	.84	.84	.83	.84	.85
	Rear cylinder[2]	.77	.78	.81	.79	.78	.78	.78	.78	.77	.78	.77	.78	.77	.76	.77	.78
Topmost fin on exhaust side of heads	Front cylinder[3]	.86	.86	.89	.88	.89	.88	.87	.89	.86	.86	.87	.85	.86	.84	.85	.86
	Rear cylinder[4]	.78	.80	.82	.80	.80	.79	.80	.80	.78	.79	.80	.79	.81	.80	.80	.79
Lowest fin on exhaust side of barrels	Front cylinder[3]	.67	.69	.70	.68	.69	.68	.68	.66	.66	.67	.66	.69	.70	.67	.71	.69
	Rear cylinder[4]	.64	.66	.67	.66	.67	.66	.66	.65	.64	.68	.65	.64	.65	.64	.64	.65

[1] Based on cylinders 6 and 10.
[2] Based on cylinder 1.
[3] Based on cylinder 4.
[4] Based on cylinder 3.
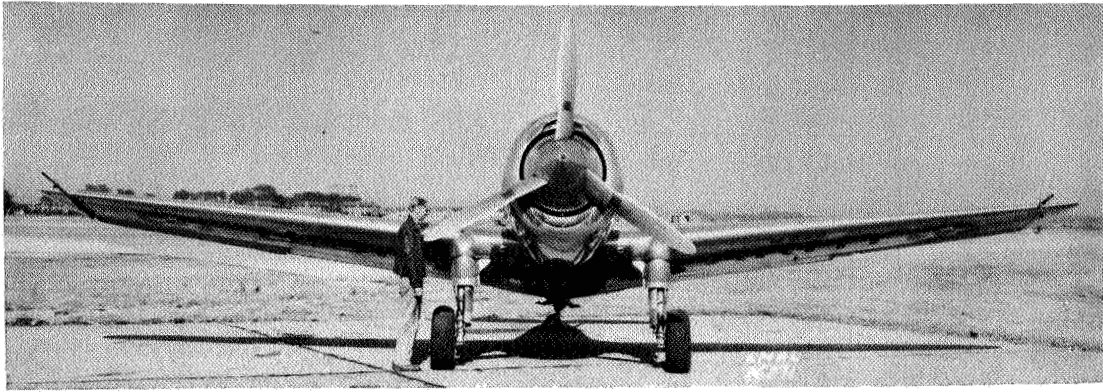
Figure 1 ‐ Front view of XP‐42 airplane with ehort-nose high-inlet-velocity cowling.
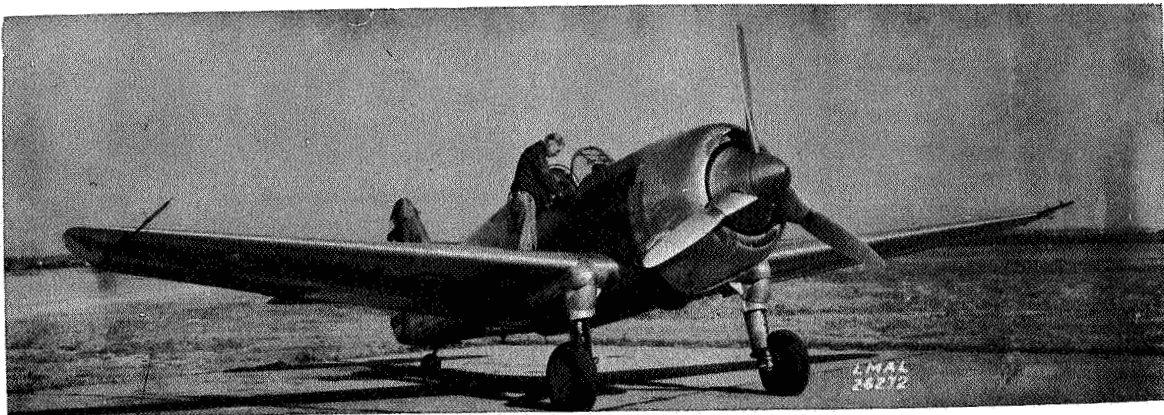
Figure 2 ‐ Three-quarter front view of the XP‐42 airplane with short-nose high-inlet-velocity cowling.
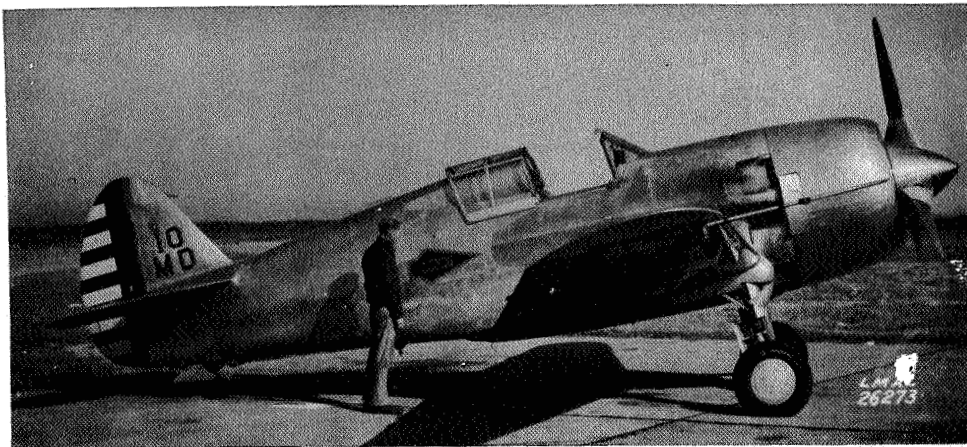
Figure 3.- Side view of the XP‐42 airplane with short-nose high-inlet-velocity cowling.

L-383
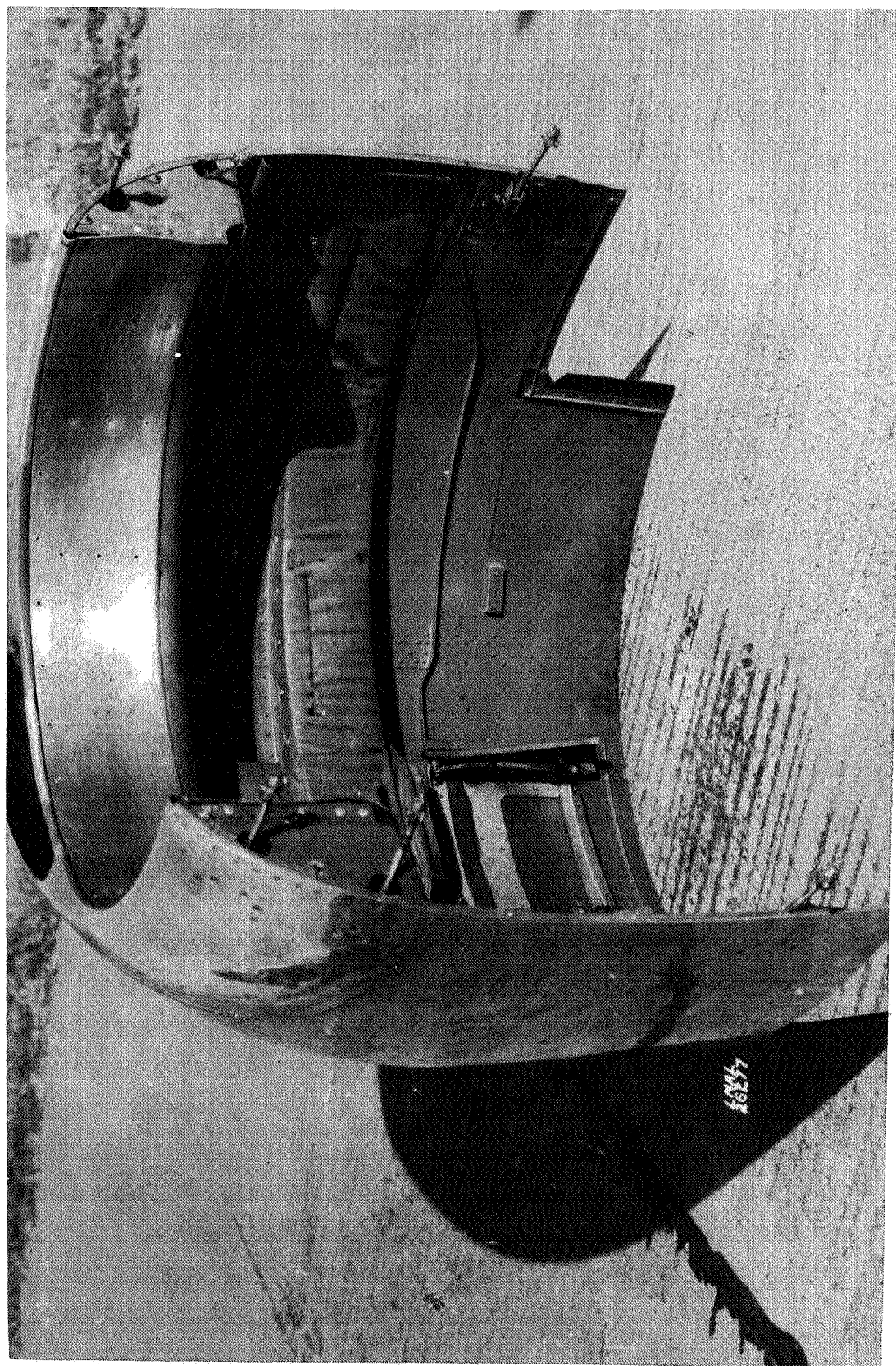
Figure 4.- Upper part of short-nose high-inlet-velocity cowling.
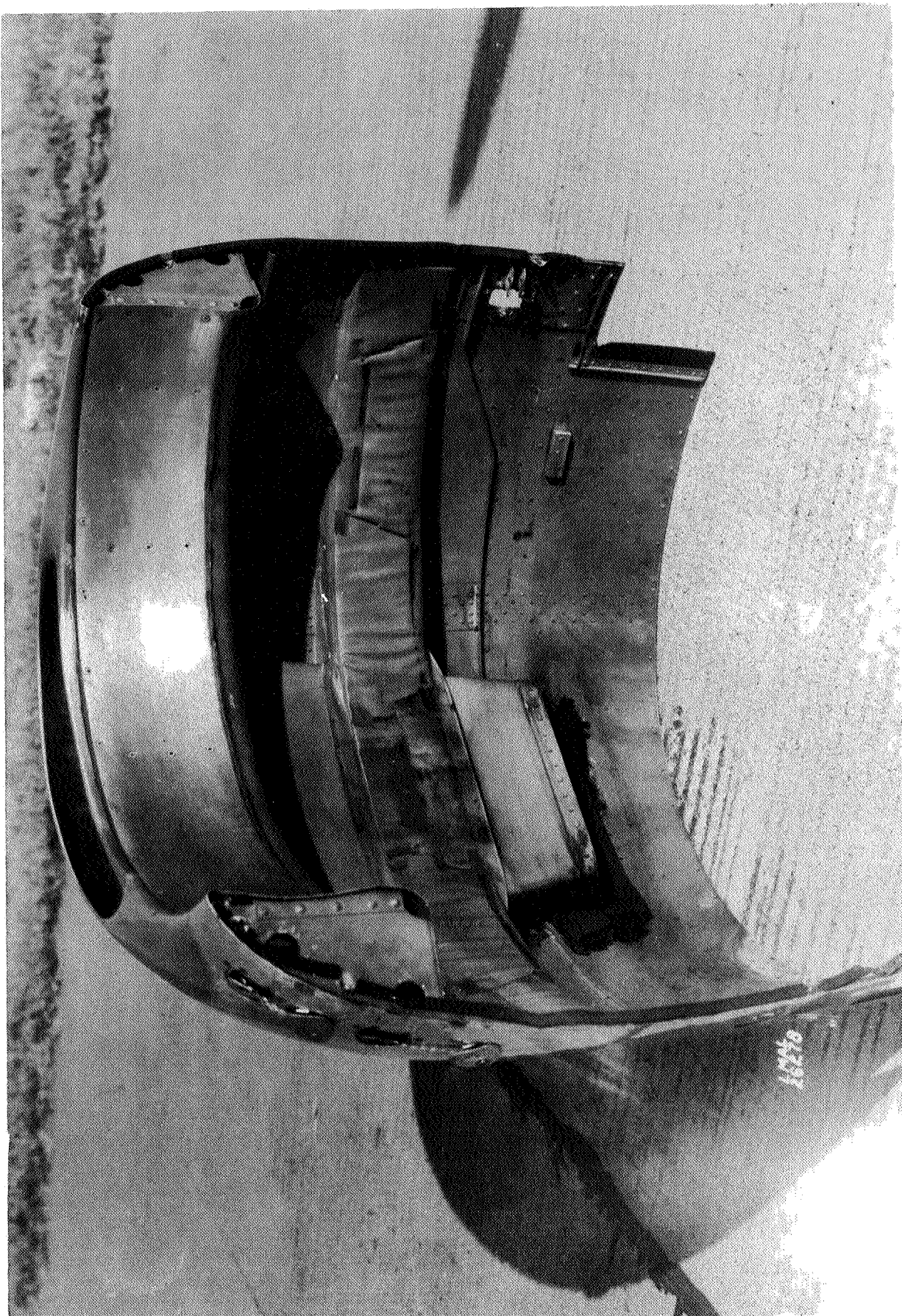
Figure 5.- Lower part of short-nose high-inlet-velocity cowling.

Fig. 6

IMPACT TUBES IN FINS ON CYL.
1,3,4,6,7,9,10,12,&14

ADDITIONAL IMPACT TUBES IN
FINS ON CYL 3 & 4

(MEASURE WITH 20ᵗʰˢ
OF AN INCH)

D.FT. CURTISS HOLLOW
STEEL BLADE. 512 cc 1.5

29° TO CHORD LINE
AT 42" STATION.

SECTION A-A

FIG. 6 XP-42 SHORT NOSE HIGH
INLET SPEED COWLING.

Fig. 7
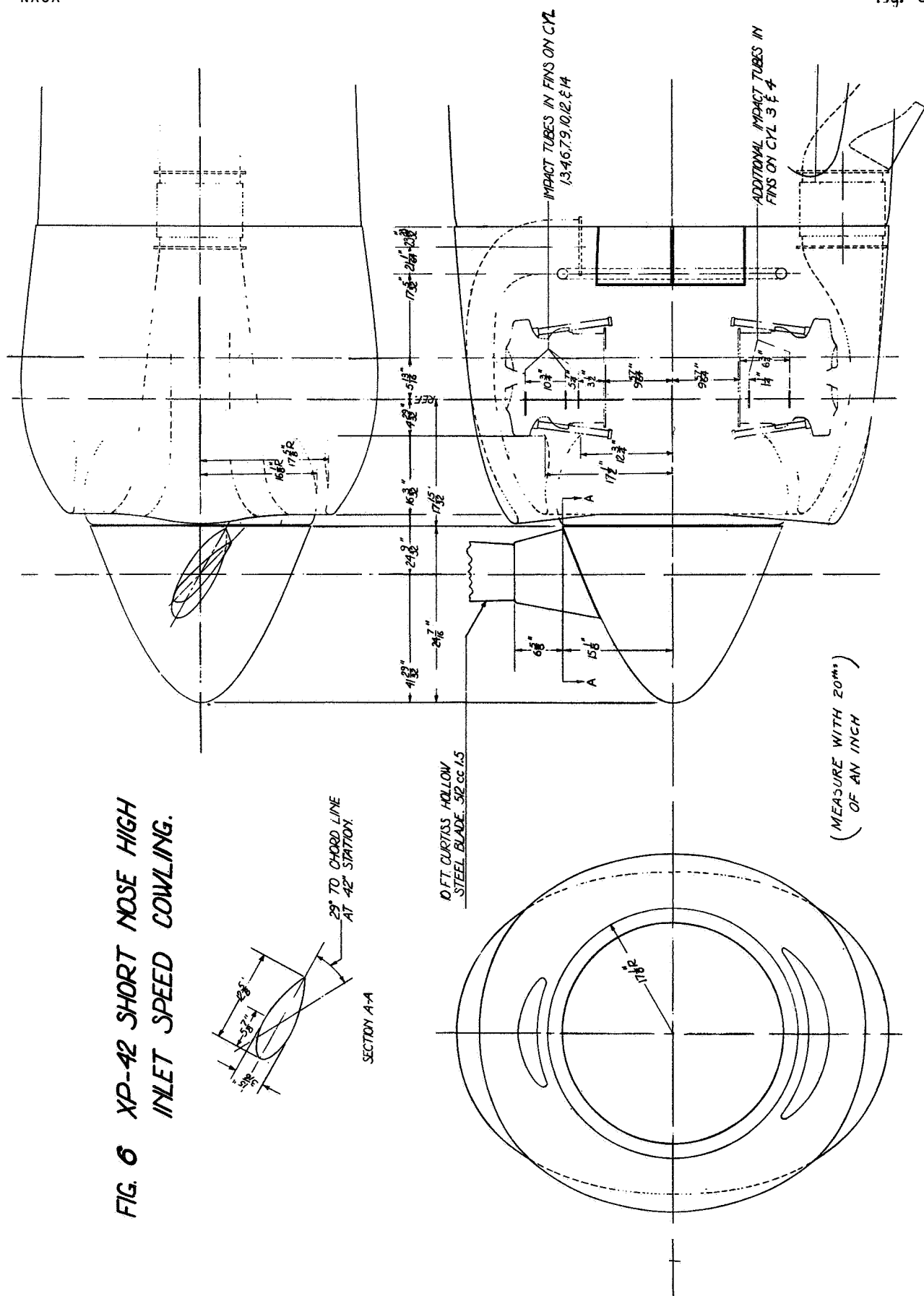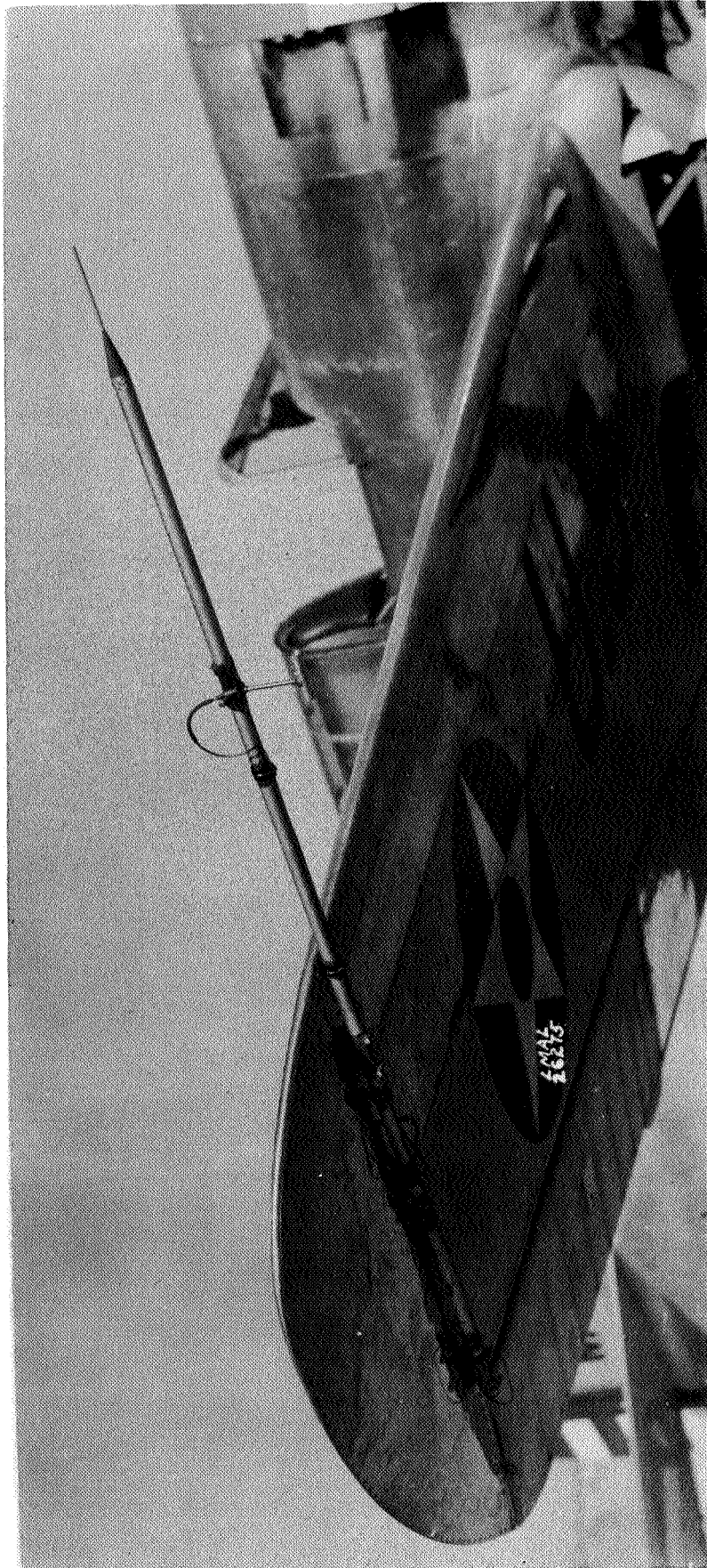
Figure 7.- Airspeed boom on right wing.
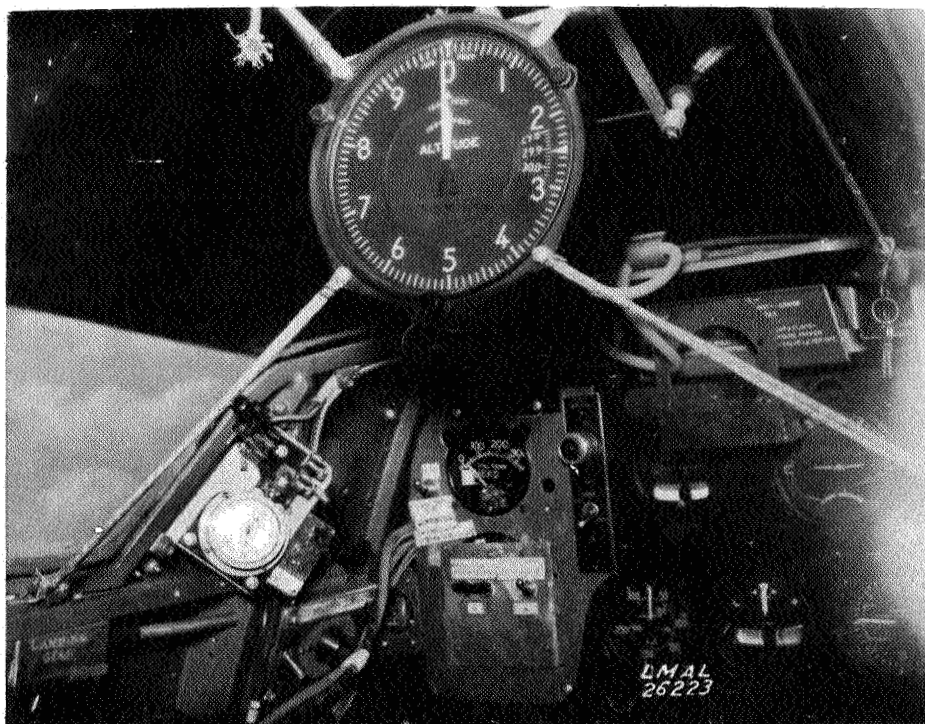
Figure 8.- Sensitive altimeter used in calibrating airspeed head.
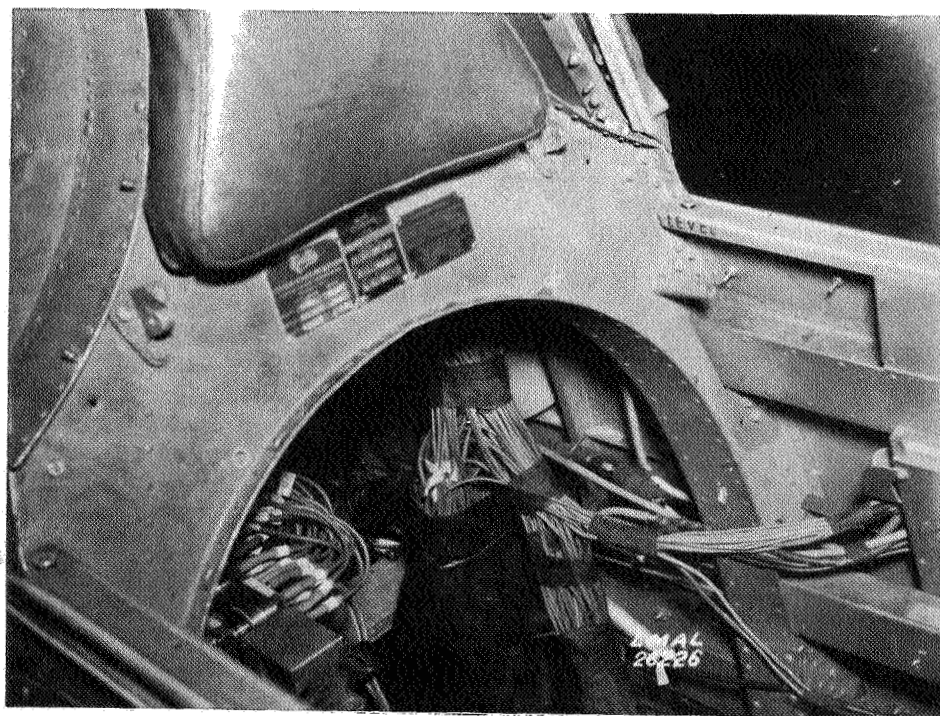
Figure 9.- Thermocouple leads *to* cold-junction box.

Figure 10.- Free-air thermocouple and vapor-pressure
thermometer.
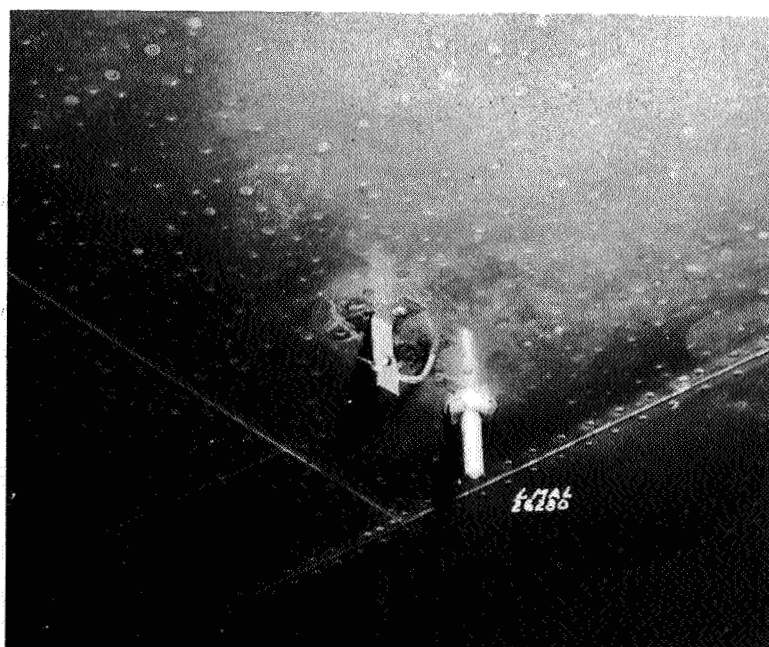
Figure 11.- Free-air thermocouple and resistance-bulb
thermometer
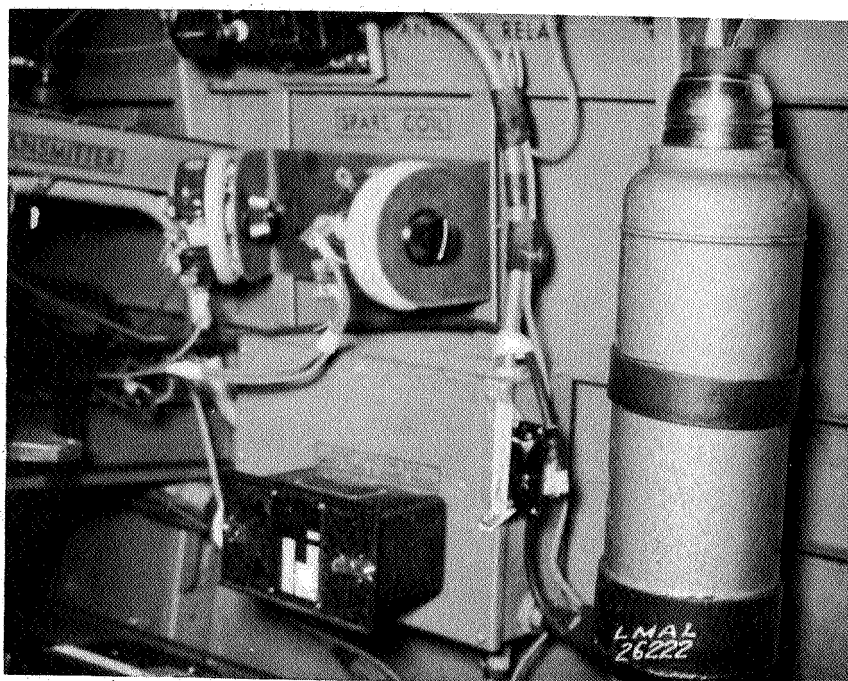
Figure 12.– Thermos bottle used as hot junction.
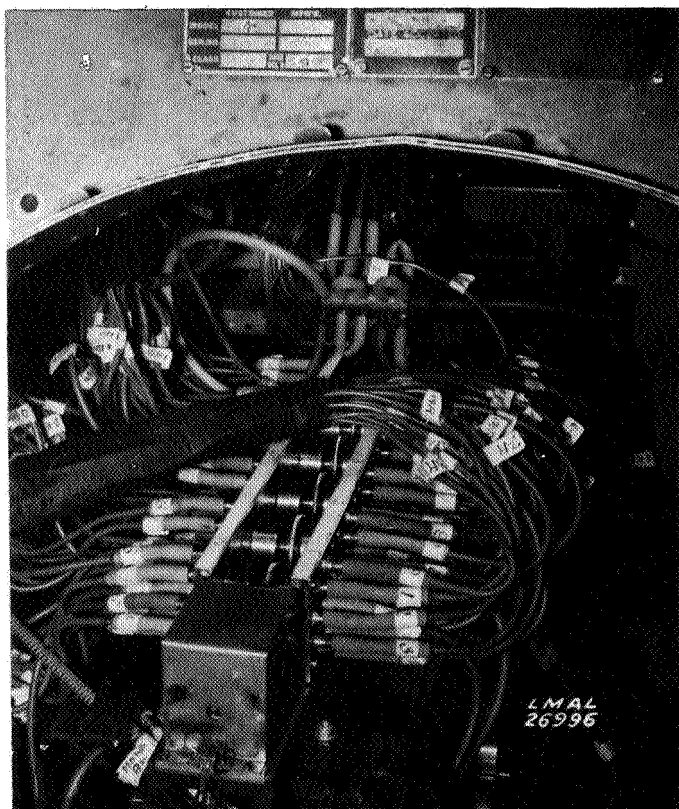
Figure 13.–
Pressure-
switch
installation
over
manometer.

L-353
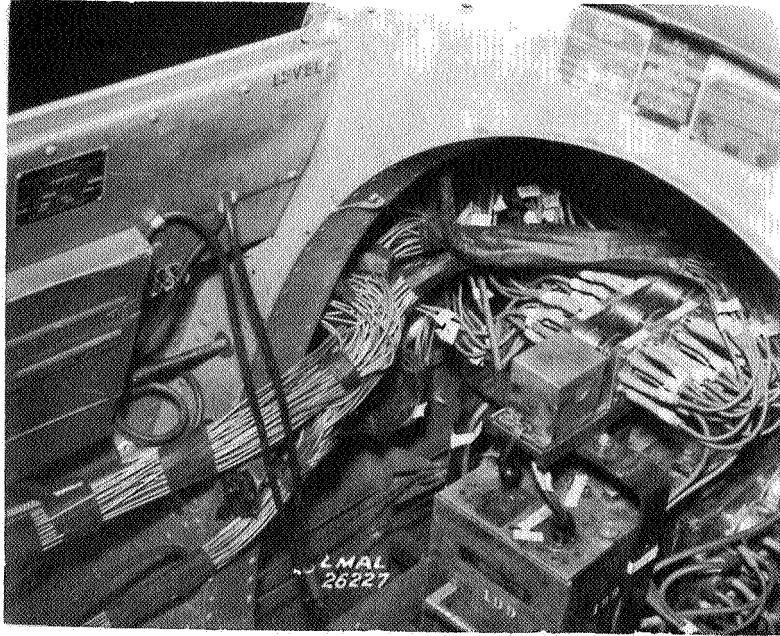
Figure 14.-
Manometer
and
pressure-
switch
installation.

Figure 17.-
Rear part
of
carburetor
duct,
showing
pressure
rakes.
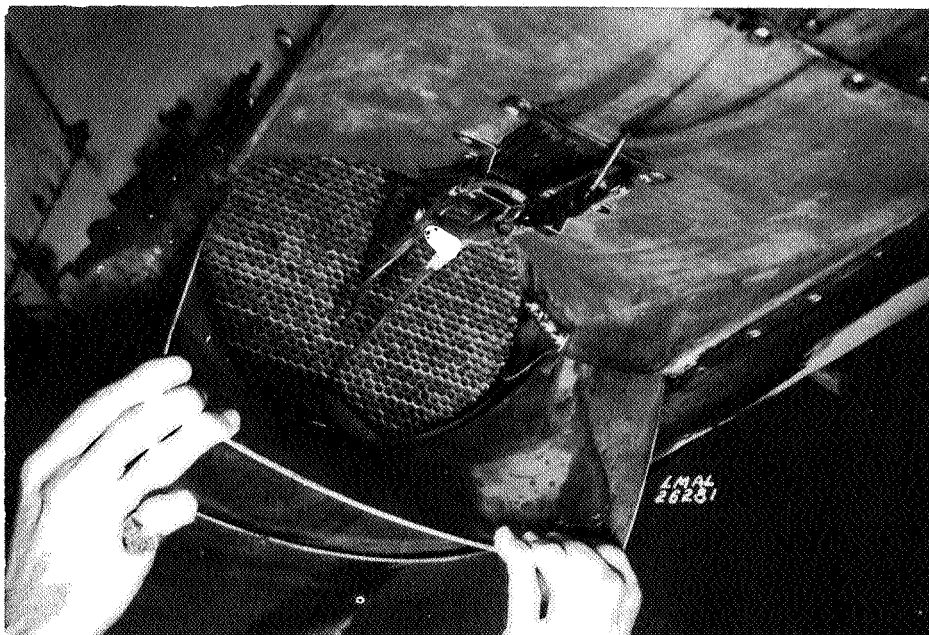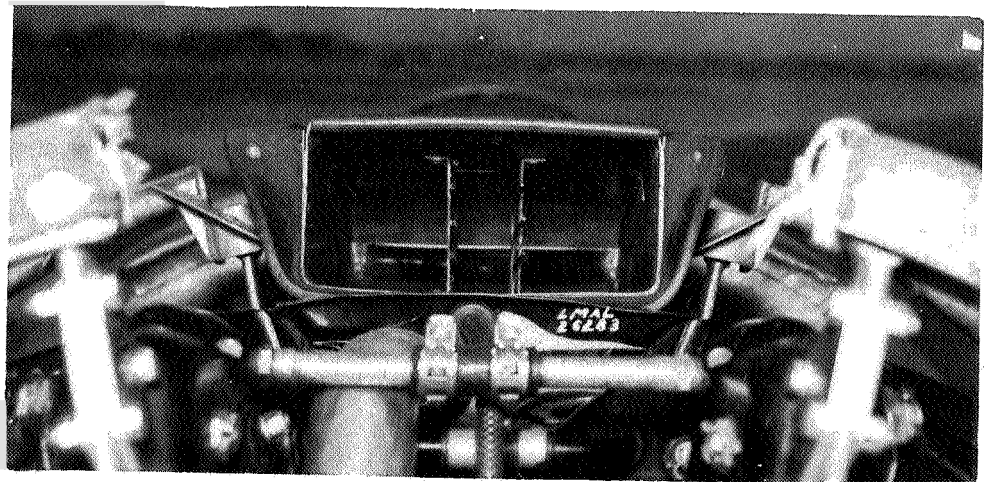
Figure 19.-
Rear
of
oil
cooler.
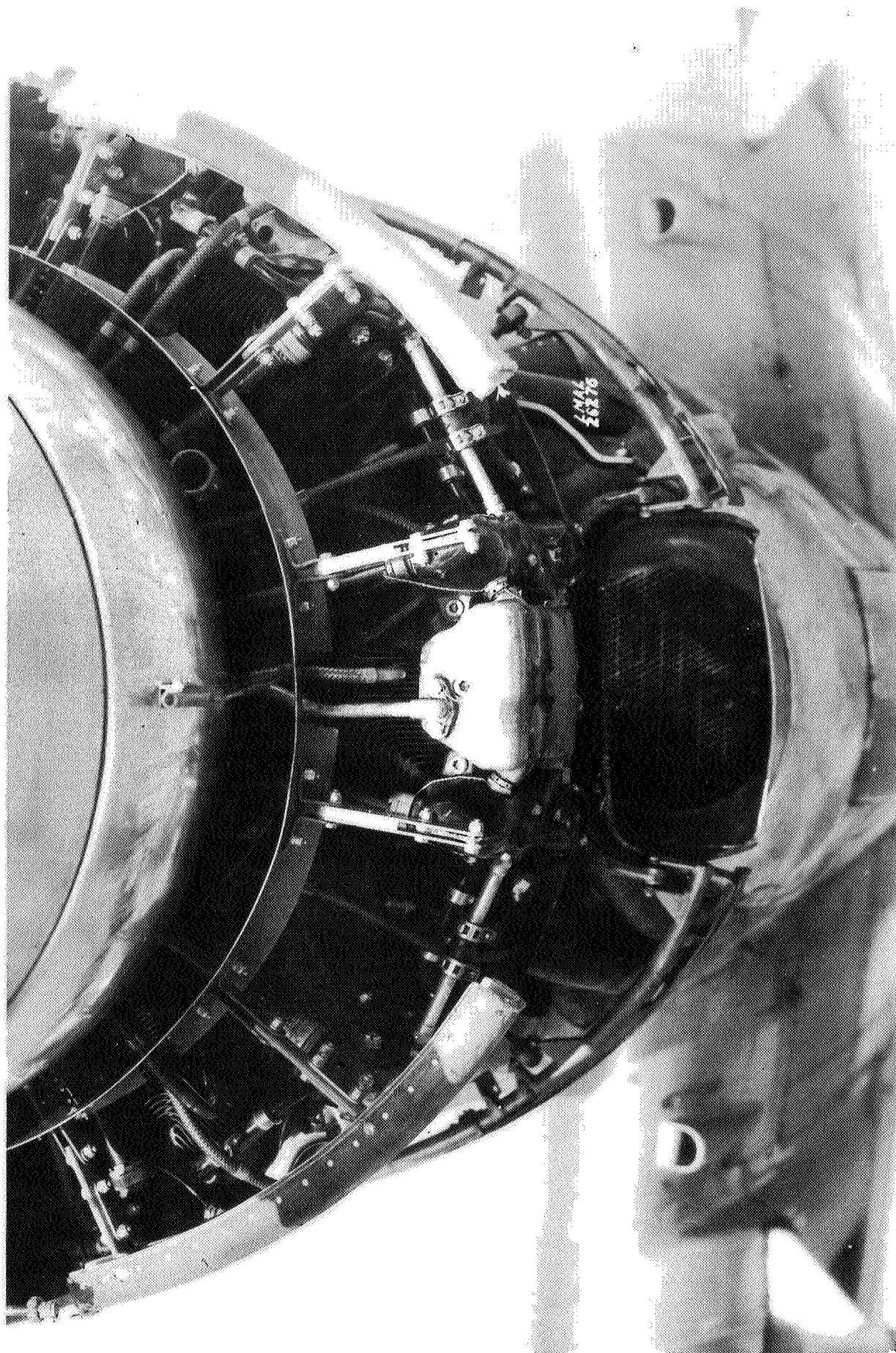
Figure 15.- Front of engine with cowling removed, showing right and left pressure rakes in annulus.

L-383
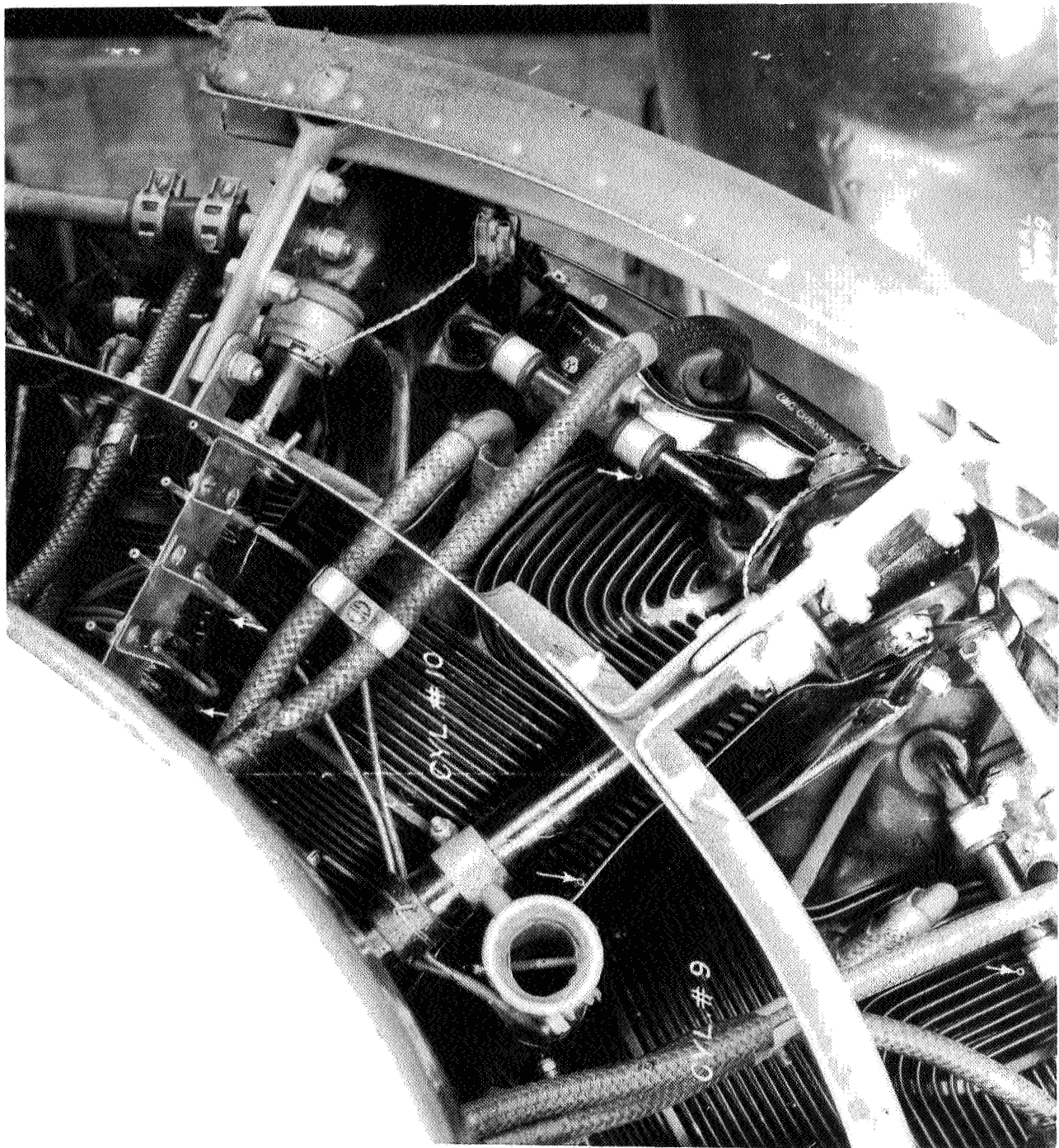
Figure 16.- Pressure tubes in baffles of cylinder 10.
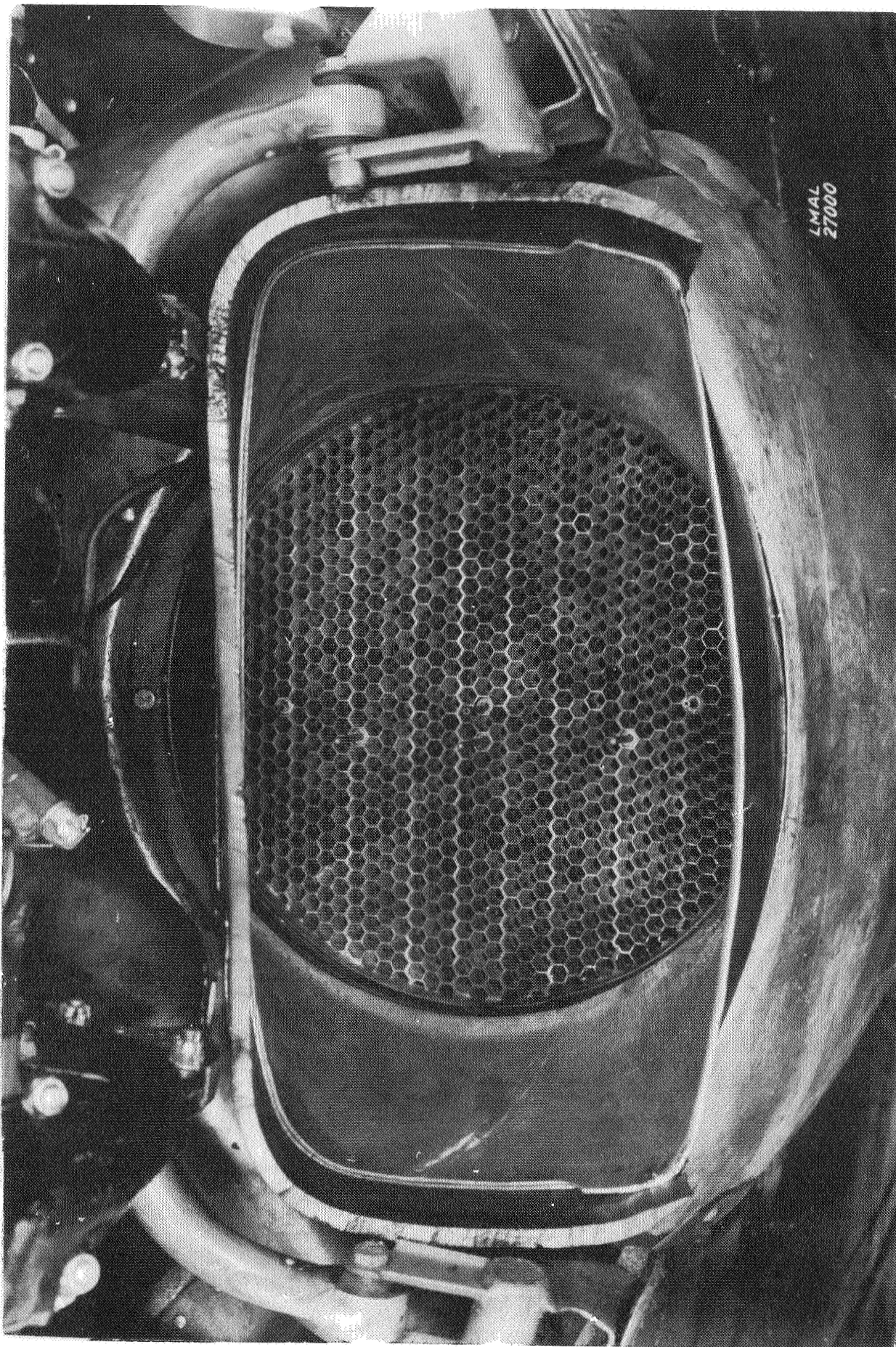
Figure 18.- Face of oil cooler, showing pressure tubes.

Fig. 20
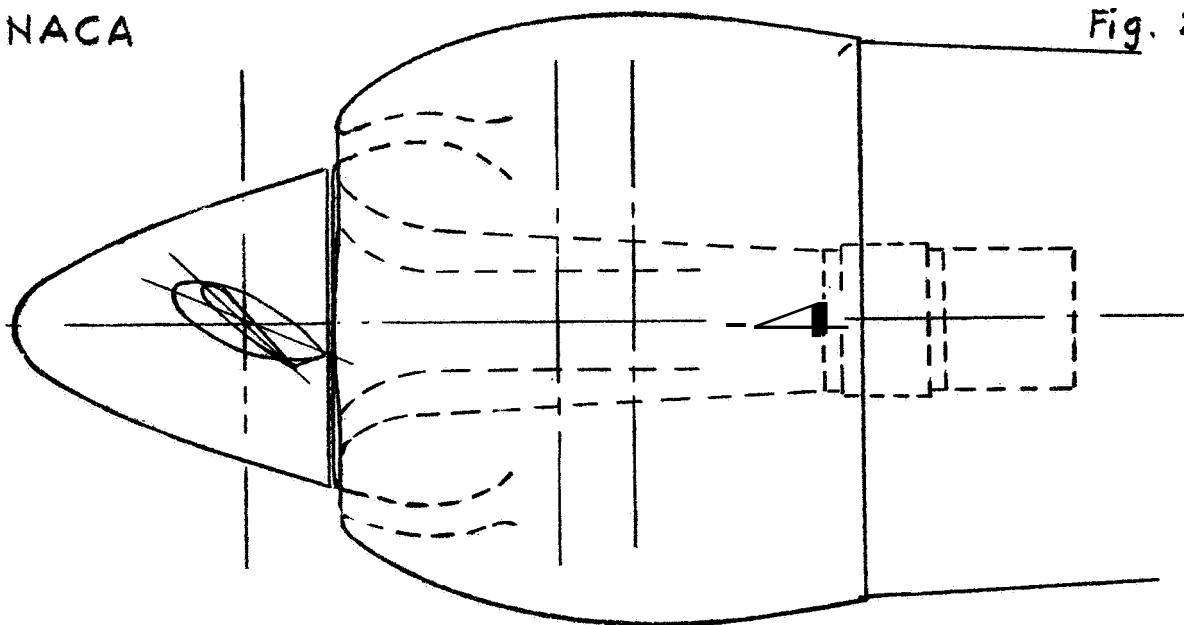
TOR VIEW

1 Static & 5 impact tubes
at 0, 120°, & 240° from top
annular entrance

5 impact & 5 static tubes
along vertical & of
carb inlet duct.

& THRUST

& FRONT CYLINDERS

& REAR CYLINDERS
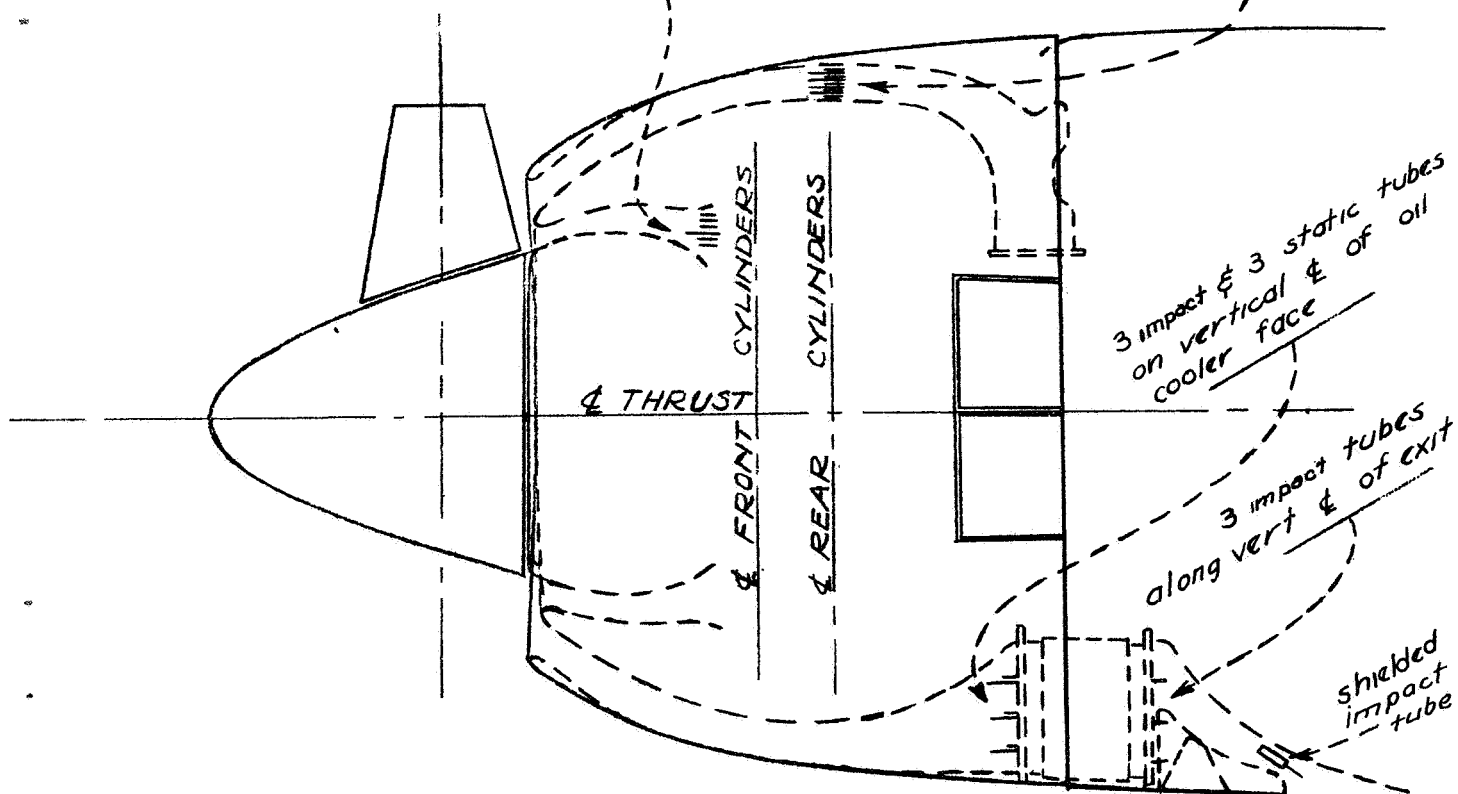
3 impact & 3 static tubes
on vertical & of oil
cooler face

3 impact tubes
along vert & of exit

shielded
impact
tube

Figure 20.–
XP-42 SHORT-NOSE HIGH-INLET VELOCITY COWLING.

L-383
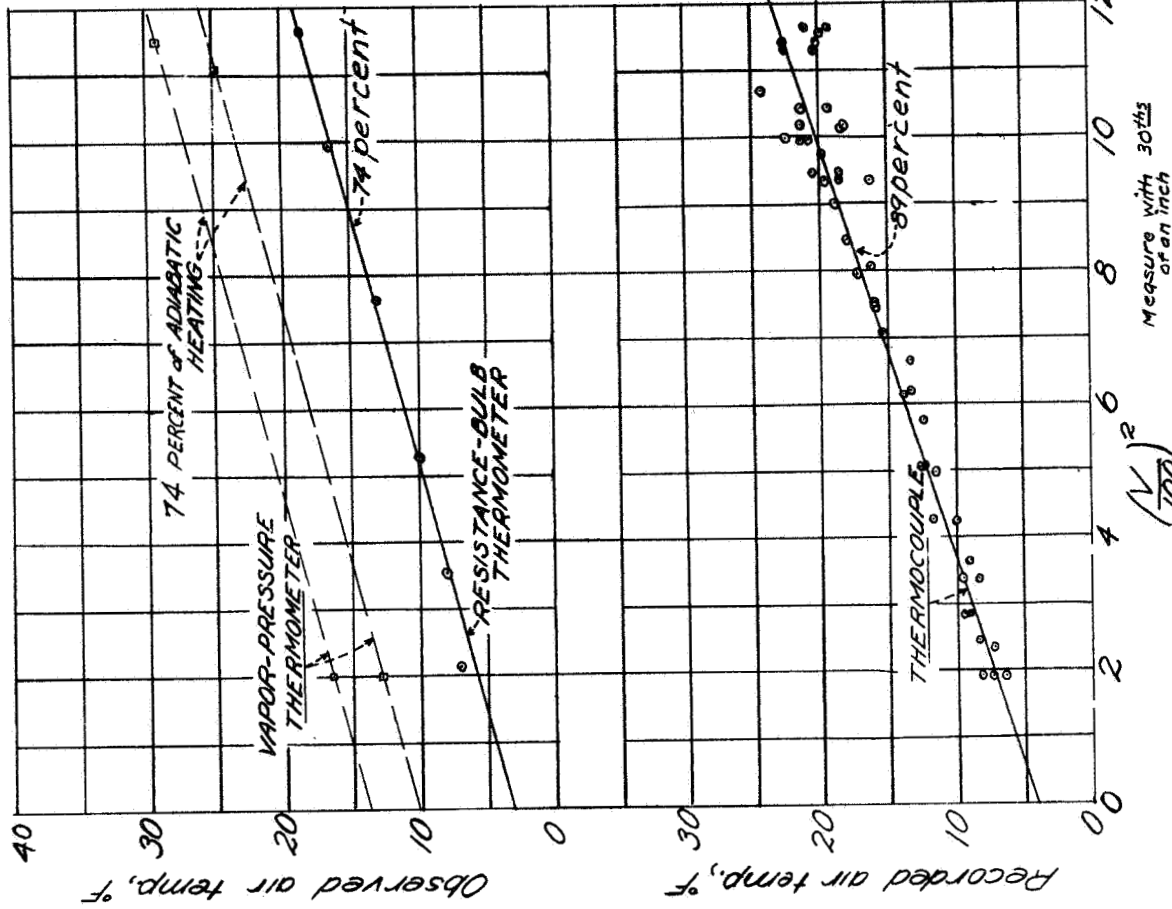
Figure 21.- Compressibility effects on free-air temperature measurements.
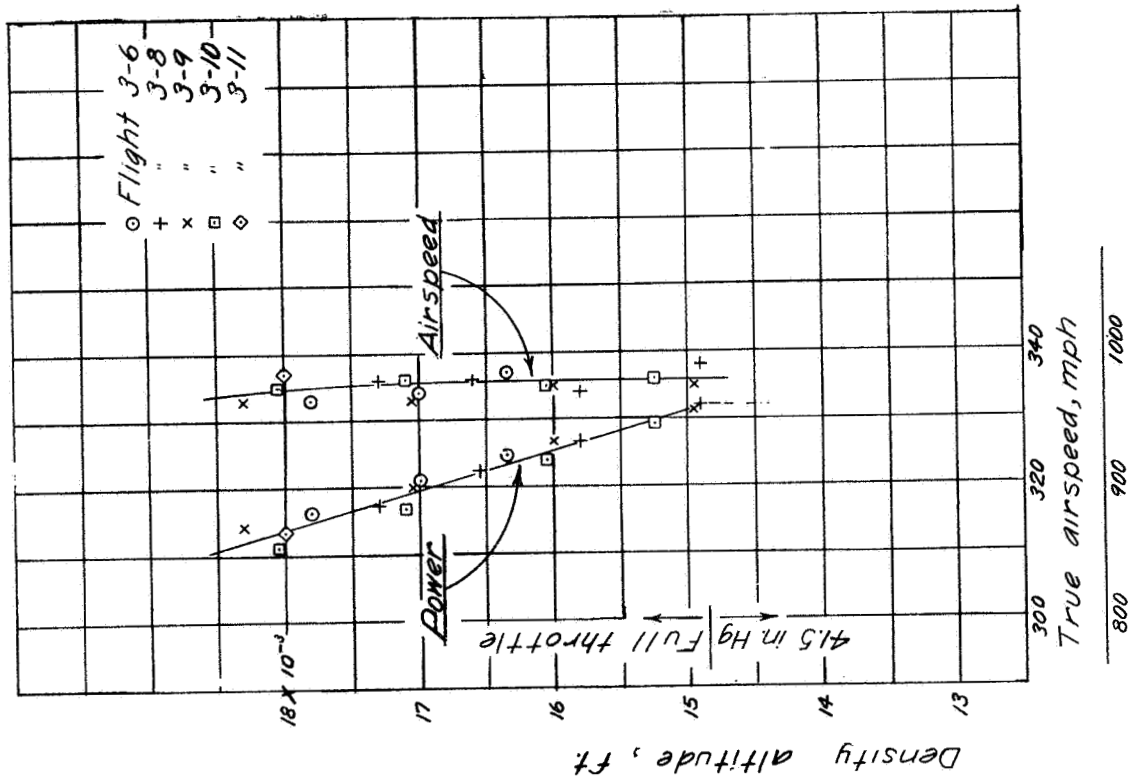
Figure 26.- Variation of airspeed and power with density altitude.

Figure 22.— Time history of flight 3-8
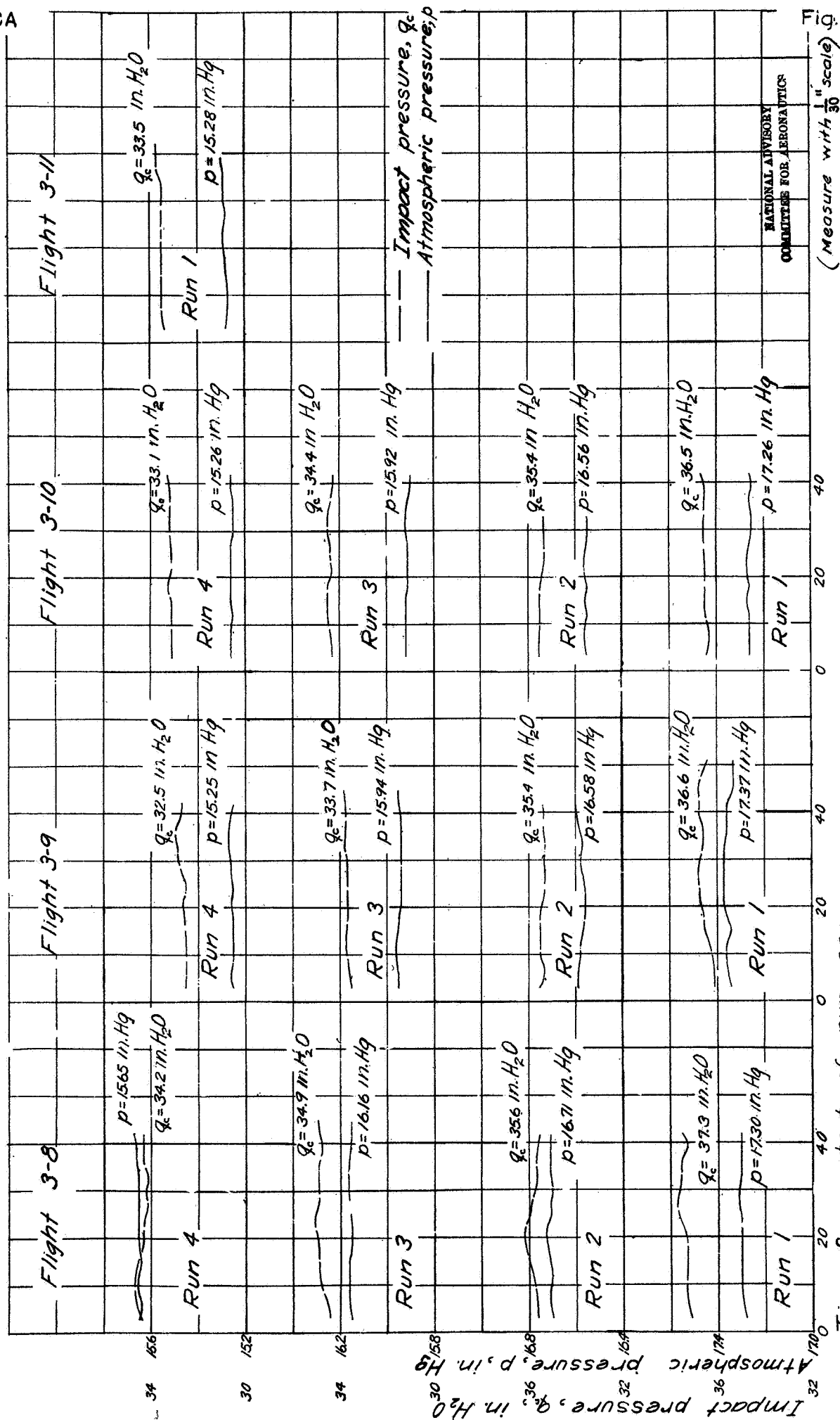
Fig. 23
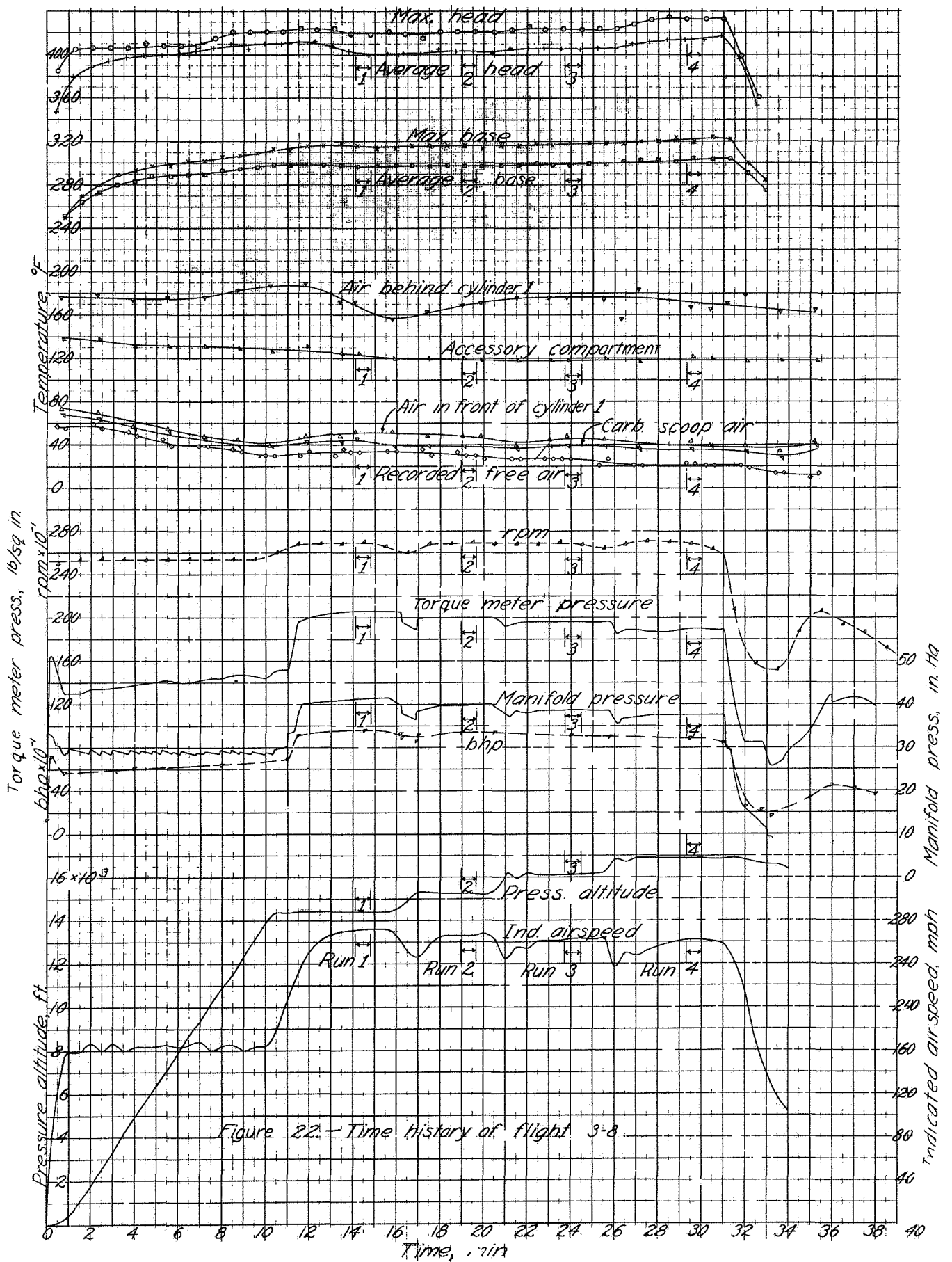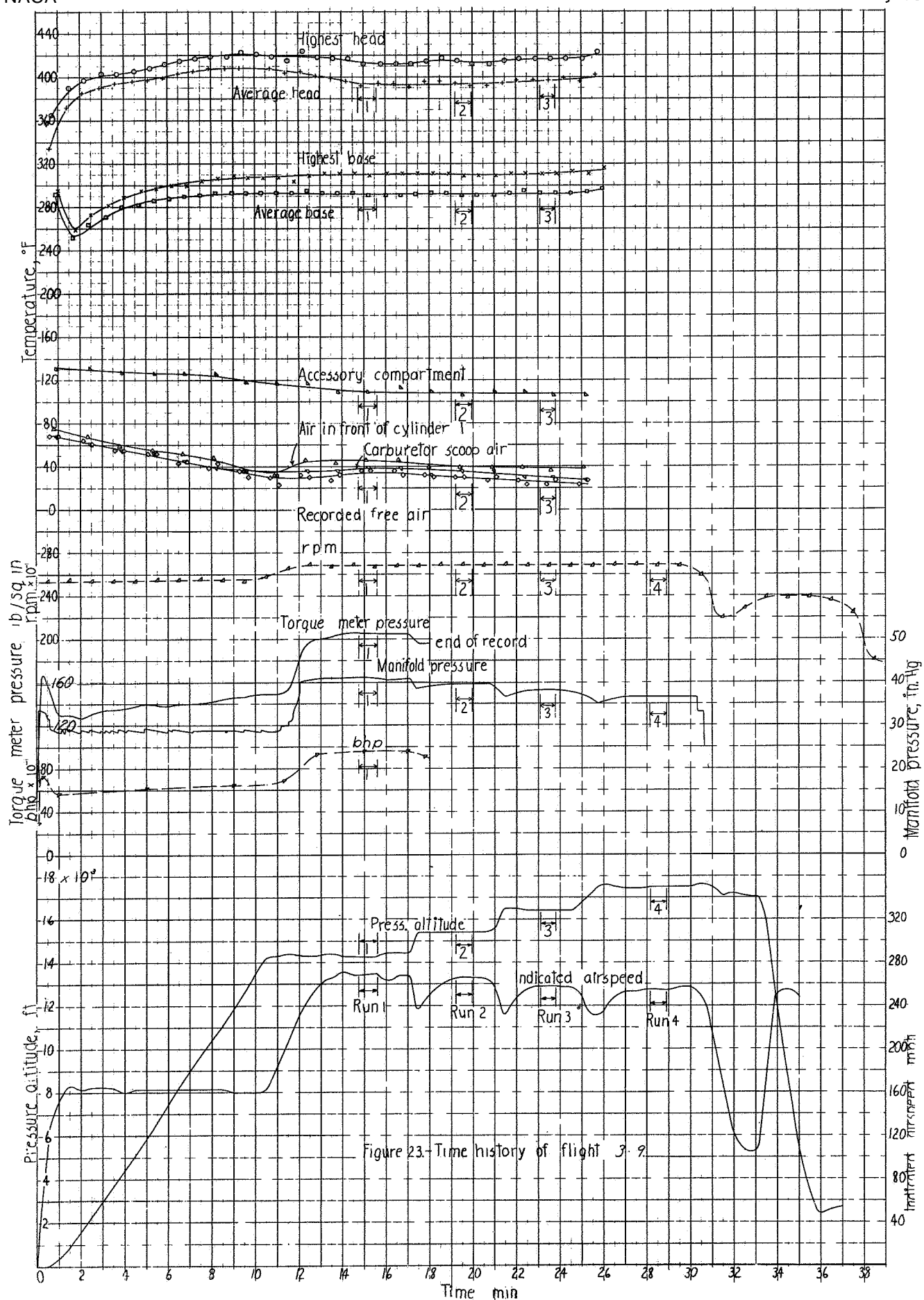
Figure 23.- Time history of flight 3 9

Fig 24
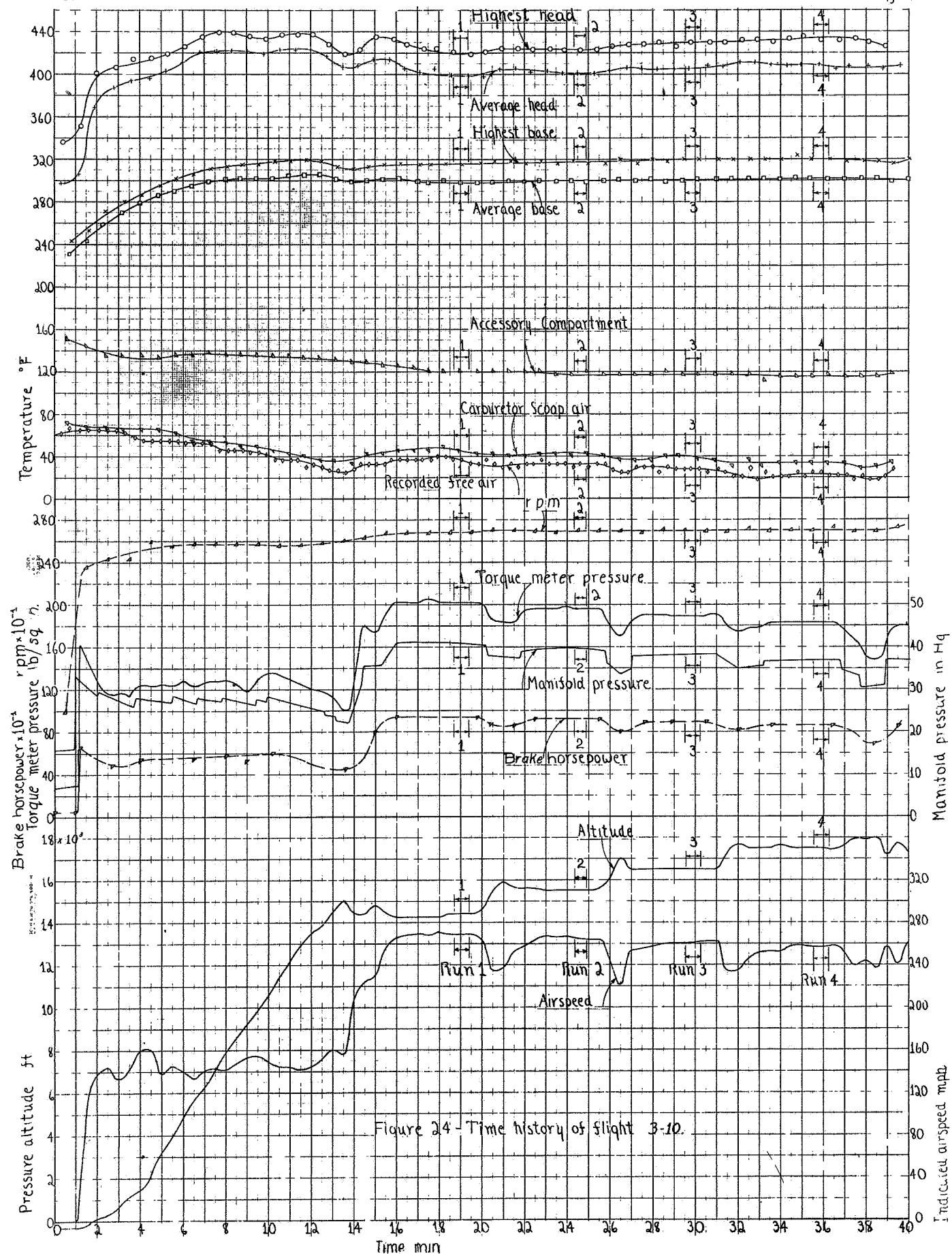
Figure 24 - Time history of flight 3-10.

NACA

Fig. 25

(Measure with $\frac{1}{30}$ scale)

L-383

Flight 3-11

Flight 3-10

Flight 3-9

Flight 3-8

$q_c = 33.5$ in. H_2O
$p = 15.28$ in. Hg
Run 1

$q_c = 33.1$ in. H_2O
$p = 15.26$ in. Hg
Run 4

$q_c = 34.4$ in. H_2O
$p = 15.92$ in. Hg
Run 3

$q_c = 35.4$ in. H_2O
$p = 16.56$ in. Hg
Run 2

$q_c = 36.5$ in. H_2O
$p = 17.26$ in. Hg
Run 1

$q_c = 32.5$ in. H_2O
$p = 15.25$ in Hg
Run 4

$q_c = 33.7$ in. H_2O
$p = 15.94$ in. Hg
Run 3

$q_c = 35.4$ in. H_2O
$p = 16.58$ in Hg
Run 2

$q_c = 36.6$ in. H_2O
$p = 17.37$ in. Hg
Run 1

$p = 15.65$ in. Hg
$q_c = 34.2$ in. H_2O
Run 4

$q_c = 34.9$ in. H_2O
$p = 16.16$ in. Hg
Run 3

$q_c = 35.6$ in. H_2O
$p = 16.71$ in. Hg
Run 2

$q_c = 37.3$ in. H_2O
$p = 17.30$ in. Hg
Run 1

Impact pressure, q_c
Atmospheric pressure, p

Time from start of run, sec.

Atmospheric pressure, p, in. Hg

Impact pressure, q_c, in. H_2O

Figure 25 — Time histories of atmospheric and impact pressures during high speed runs
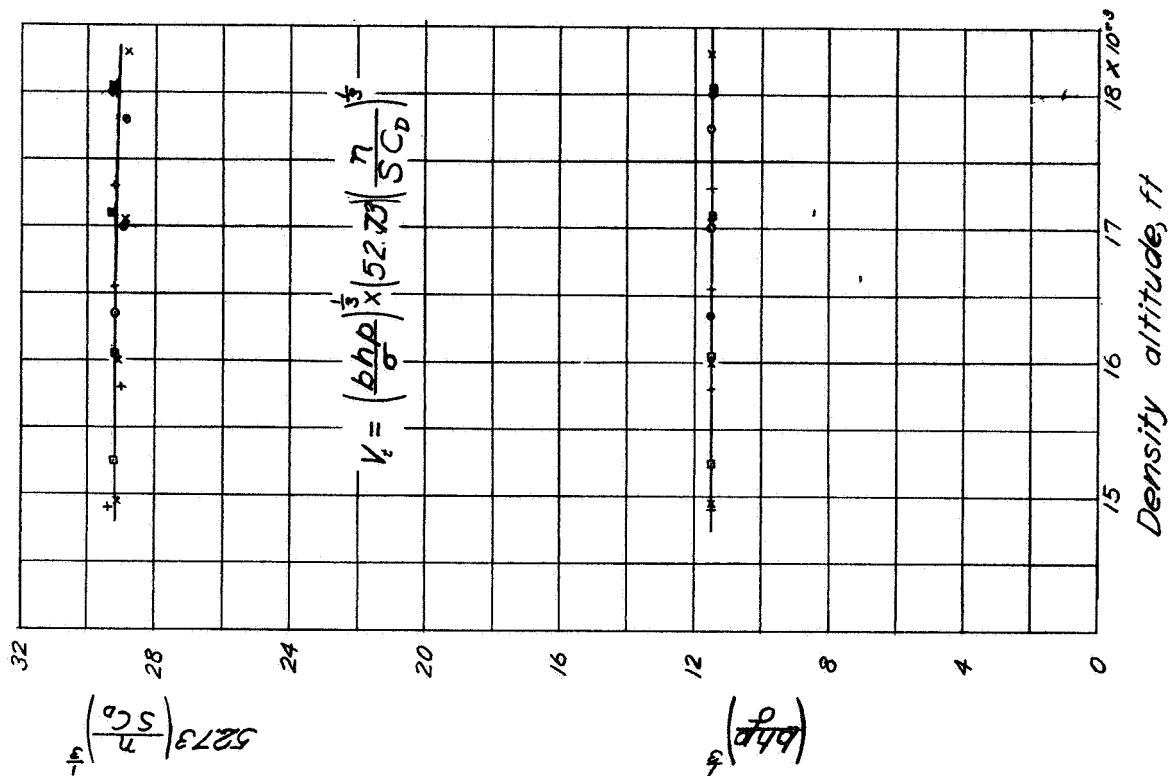
Figure 27.- Analysis of high-speed performance.

$$V_t = \left(\frac{bhp}{\sigma}\right)^{\frac{1}{3}} \times (52.73)\left(\frac{n}{SC_D}\right)^{\frac{1}{3}}$$

(Measure with 30ths of an inch)

⊙ XP-42   SHORT NOSE, ORIGINAL CUFFS
× P-42   SHORT NOSE, MODIFIED CUFFS
+ P-36A
▣ P-40C
△ XP-42   LONG NOSE

$$\left(\frac{V}{52.73}\right)^3 = \left(\frac{bhp}{\sigma}\right)\left(\frac{n}{SC_D}\right)$$

Measure with 30ths
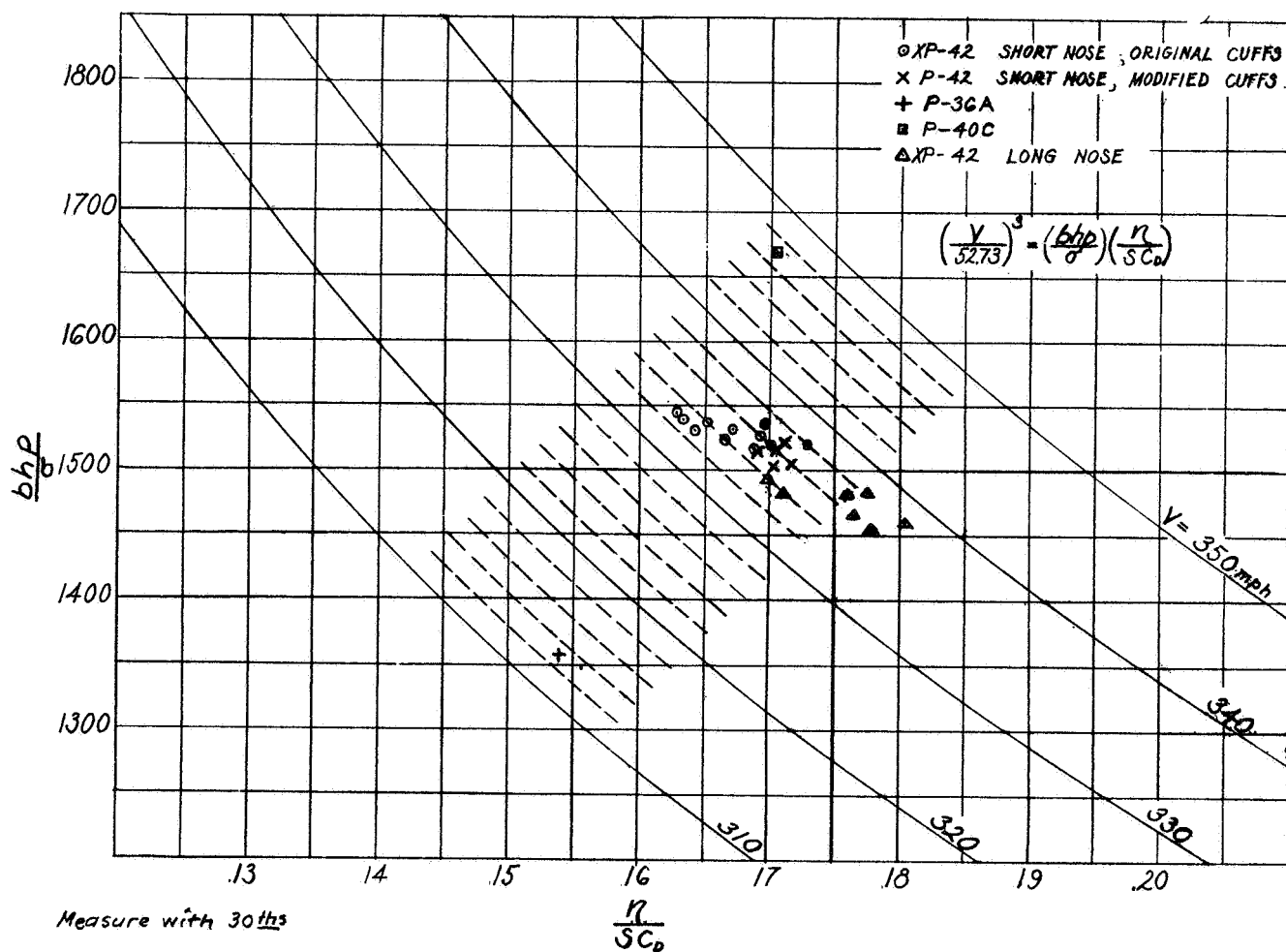
Figure 28.- Comparison of high-speed performance on several airplanes.
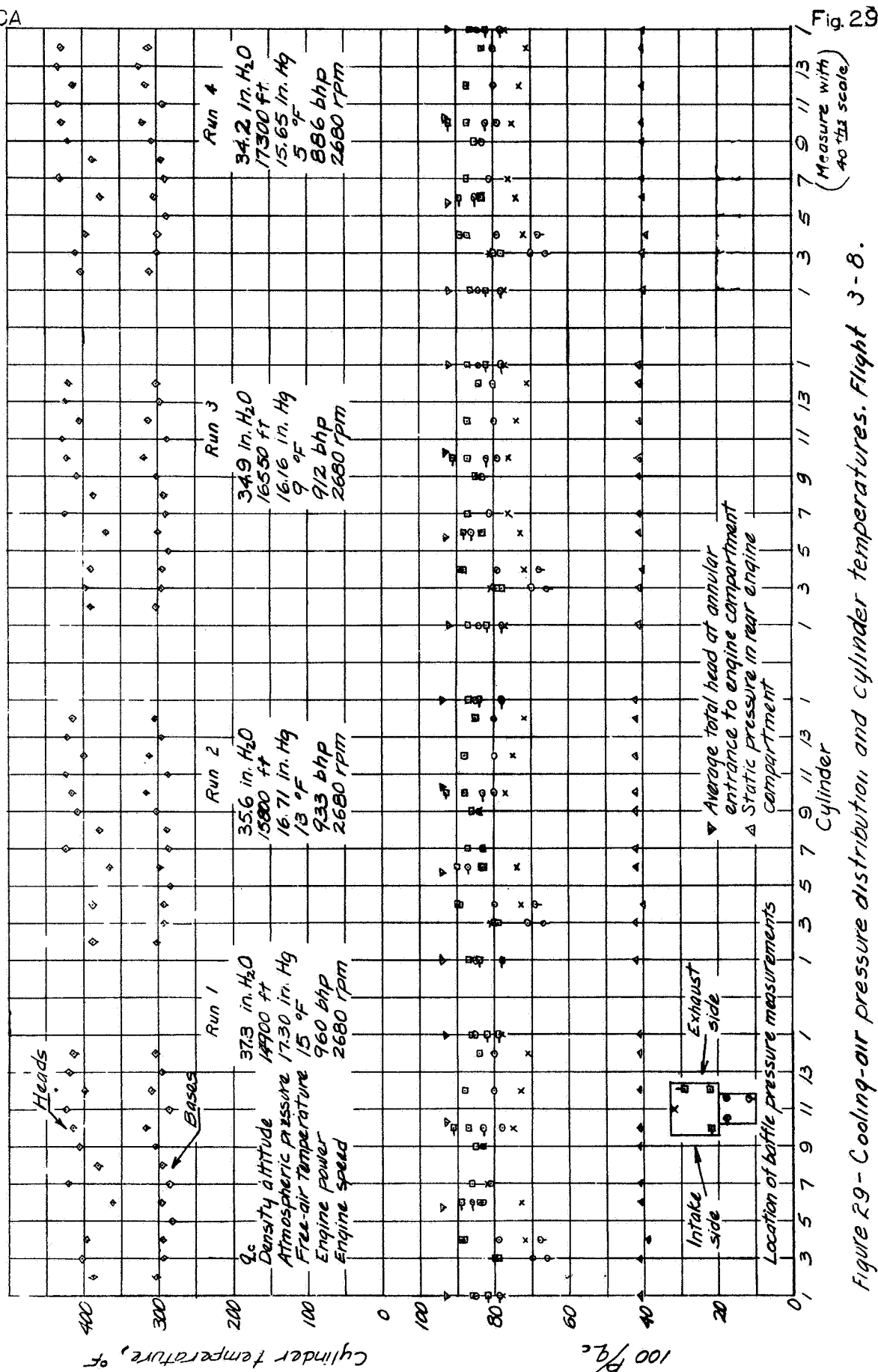
Figure 29 - Cooling-air pressure distribution and cylinder temperatures. Flight 3 - 8.

Fig. 30
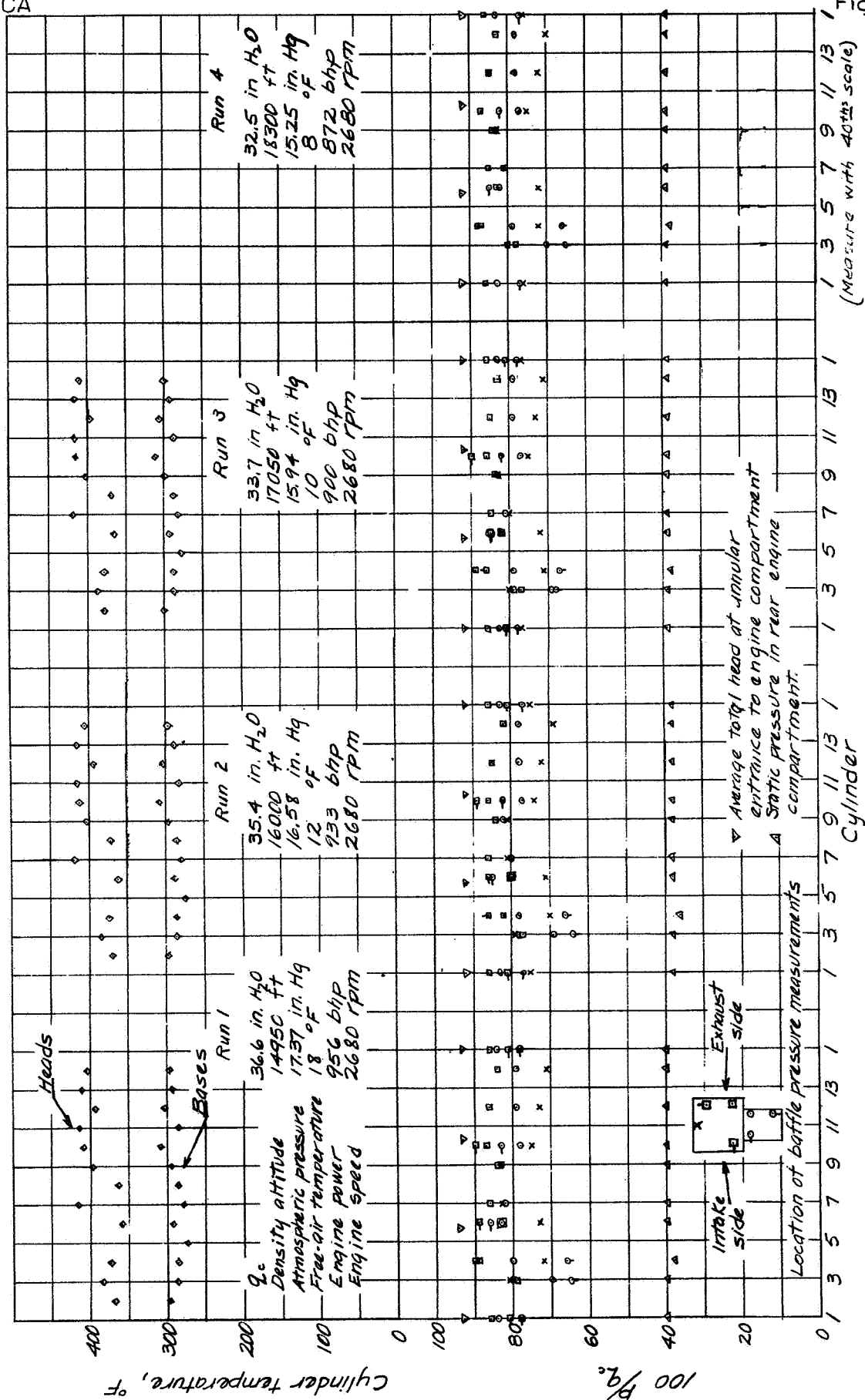
Figure 30 - Cooling-air pressure distribution and cylinder temperatures Flight 3-9
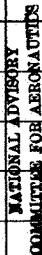
Fig. 31

Figure 31 - Cooling-air pressure distribution and cylinder temperature   Flight 3-10.
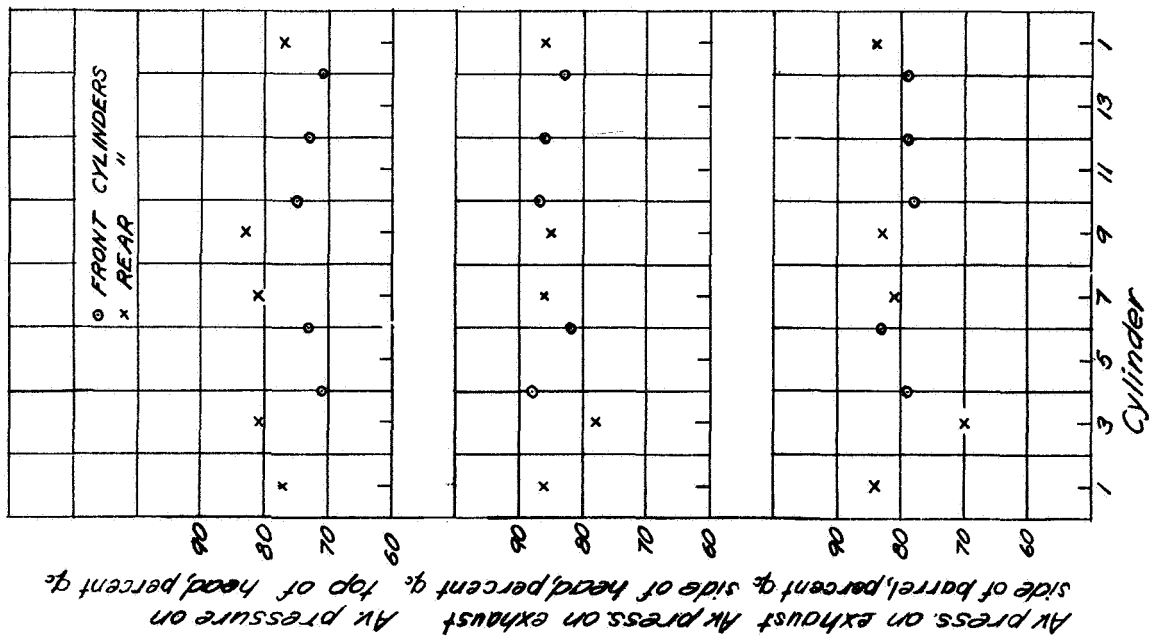
L-383
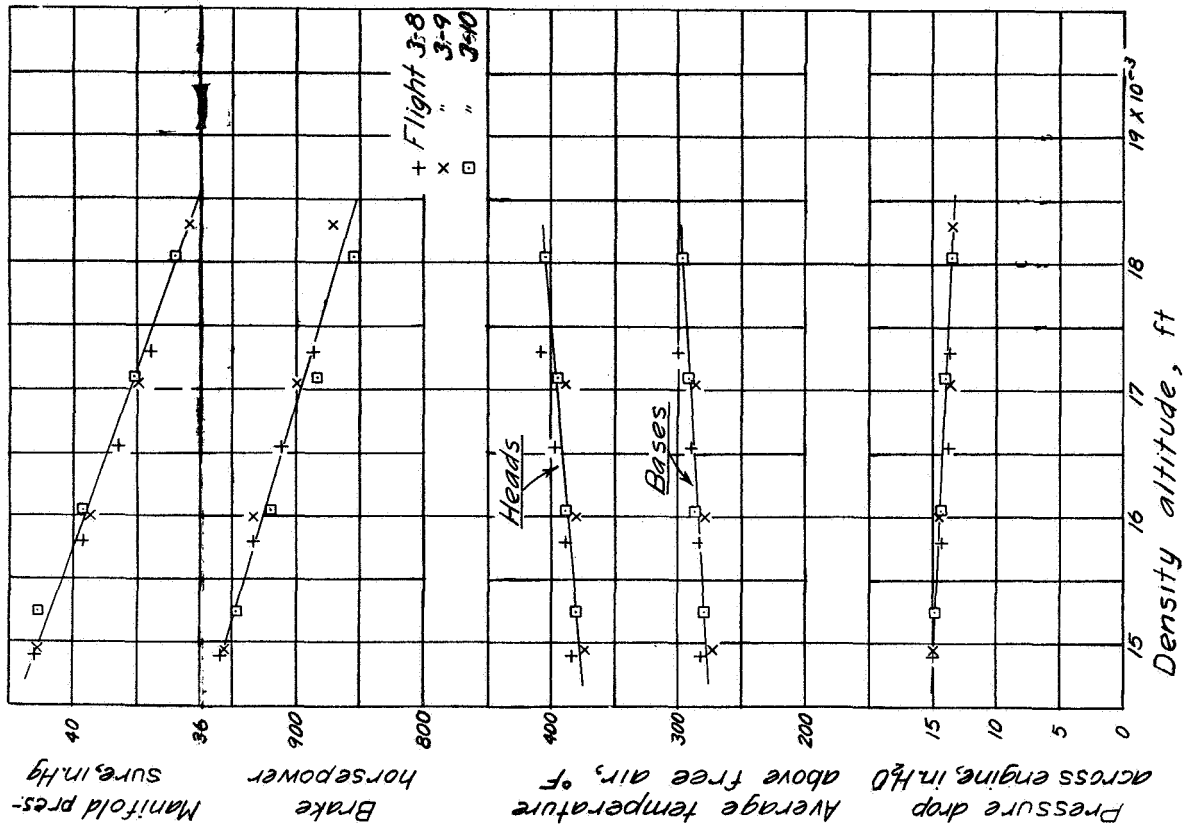
Figure 33.— Effect of altitude on cooling.

Figure 32.— Pressures at several locations on individual
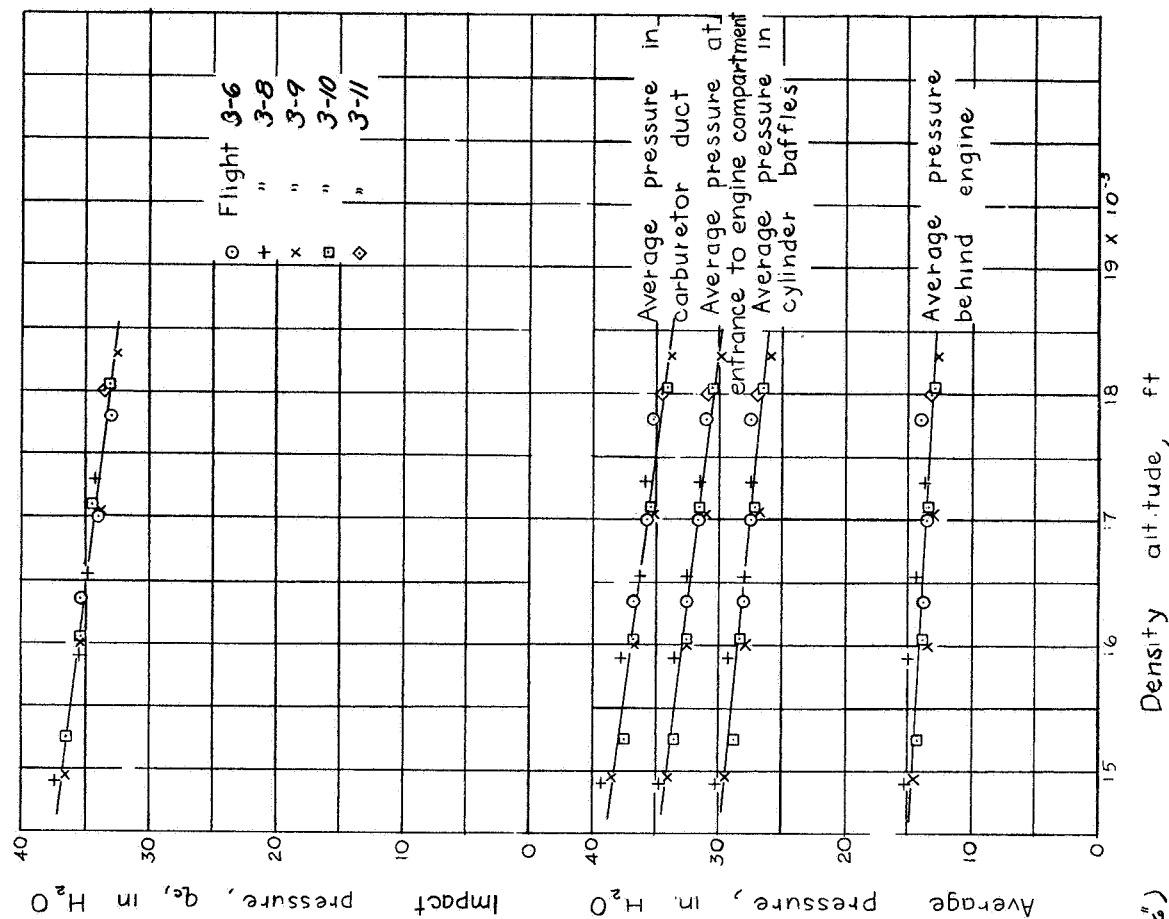cylinders, averaged for all high-speed runs.

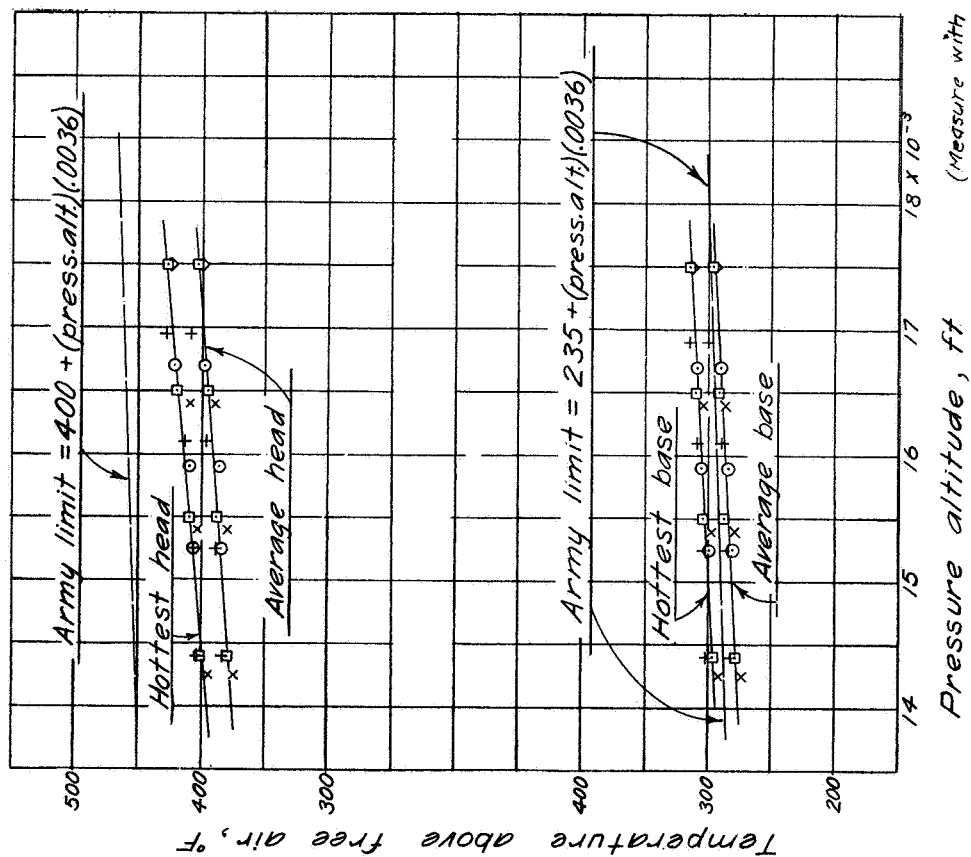Figure 35.— Comparison of average induction and cooling-air pressures at several locations.

Figure 34.— Comparison of cylinder temperature with Army limits.
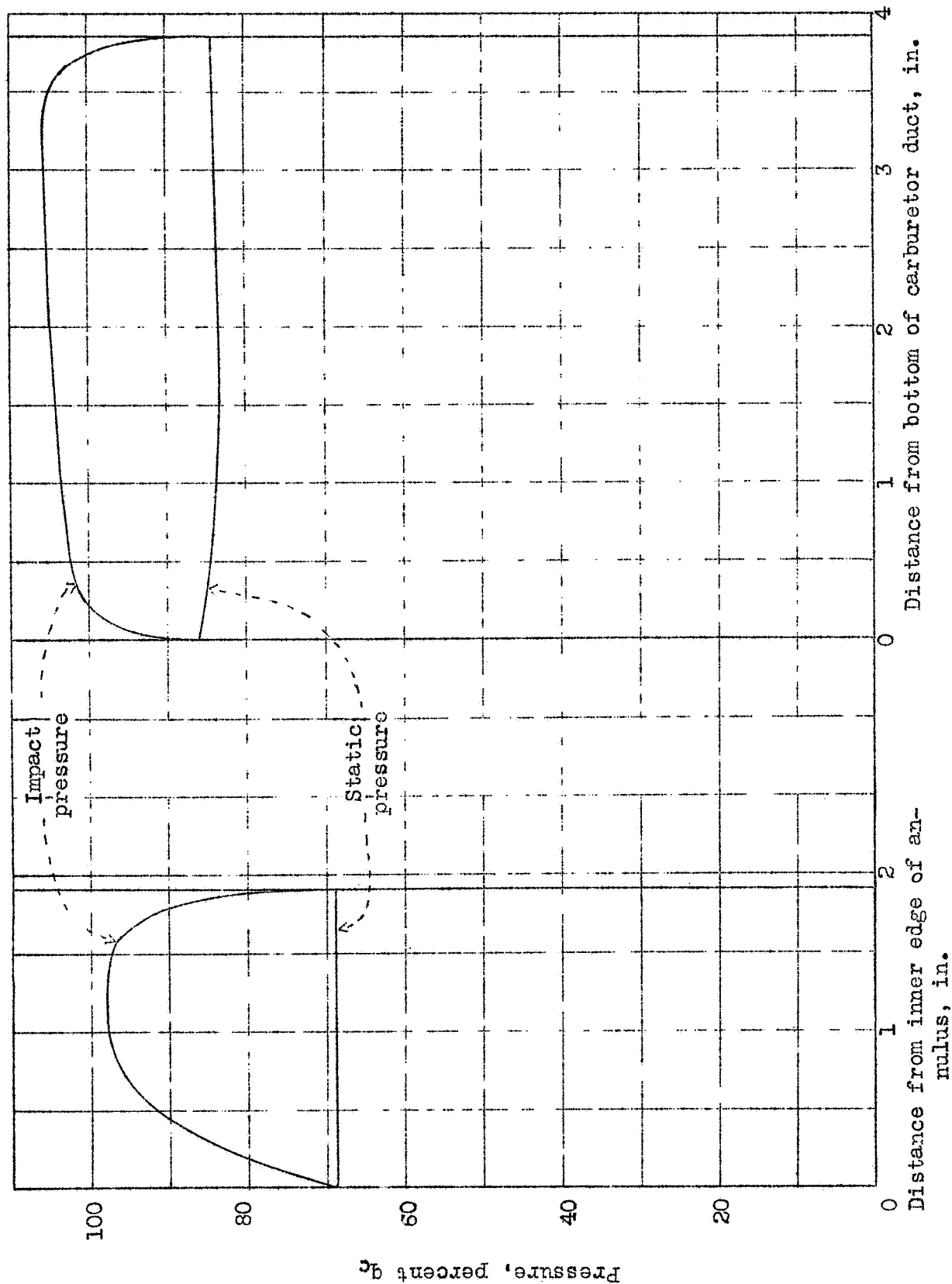
Fig. 36

Figure 36.- Average pressure distribution in annular entrance to engine compartment and in carburetor duct.